Ecotoxicology and Environmental Safety 286 (2024) 117214

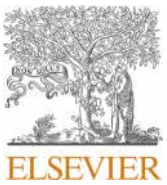

Contents lists available at ScienceDirect

Ecotoxicology and Environmental Safety

journal homepage: www.elsevier.com/locate/ecoenv

# Bioaccumulation of polycyclic aromatic hydrocarbons and microbiota dynamics across developmental stages of the Asian tiger mosquito, *Aedes albopictus* exposed to urban pollutants

Pierre Antonelli [a], Stéphanie Grizard [a], Florence Hélène Tran [a,1], David Lejon [b], Aymeric Bellemain [b], Van [a], Patrick Mavingui [c], David Roiz [d], Frédéric Simard [d], Edwige Martin [a], Danis Abrouk [a], Aurélien Vigneron [a], Guillaume Minard [a], Claire Valiente Moro [a,*]

[a] Universite Claude Bernard Lyon 1, Laboratoire d'Ecologie Microbienne, UMR CNRS 5557, UMR INRAE 1418, VetAgrop Sup, 69622 Villeurbanne, France
[b] Rovaltain Research Company, Valence, France
[c] UMR PIMIT, Processus Infectieux en Milieu Insulaire Tropical, CNRS 9192, INSERM U1187, IRD 249, Université de La Réunion, Sainte-Clotilde, La Réunion, France
[d] MIVEGEC, Univ. Montpellier, IRD, CNRS, Montpellier, France

ARTICLE INFO

Edited by Professor Bing Yan

*Keywords:*
Polycyclic aromatic hydrocarbons
Microbiota
Mosquito
*Aedes albopictus*
Mesocosm

ABSTRACT

*Aedes albopictus* mosquitoes face numerous anthropic stressors in urban areas. These xenobiotics not only impact mosquito physiology but also shape the composition of their microbiota, which play important roles in host physiological traits. Polycyclic aromatic hydrocarbons (PAHs) are ubiquitous environmental pollutants known to alter mosquito metabolism, but no studies have yet investigated their impact on microbiota. Using a bespoke indoor mesocosm tailored for *Ae. albopictus* mosquitoes, we investigated the dynamics of bacterial communities in both mosquitoes and their larval breeding sites following chronic exposure to a cocktail of PAHs consisting of benzo[*a*]pyrene, benz[*a*]anthracene, chrysene and benzo[*b*]fluoranthene. Our findings showed that PAHs have a stage-specific effect on mosquito microbiota, with a higher impact in larvae than in adults, contributing to 12.5 % and 4.5 % of the PAHs-induced variations, respectively. The presence of PAHs in the treated mesocosm led to the enrichment of bacterial families and genera known for their ability to catabolize PAHs, such as Comamonadaceae and *Raoultella* (increasing from 19 % to 30 % and from 1.2 % to 5.6 %, respectively). Conversely, prevalent taxa found in mosquito microbiota like *Wolbachia* and *Cedecea* exhibited a reduction (decreasing from 4 % to 0.8 % and from 12.8 % to 6.4 %, respectively). This reduction could be attributed to the competitive advantage gained by PAH-degrading taxa, or it could reflect a direct sensitivity to PAH exposure. Overall, this indicates a shift in microbiota composition favoring bacteria that can thrive in a PAH-contaminated environment. PAHs persisted in the water of breeding sites only the first 45 days of the experiment. Benzo[*a*]pyrene and benzo[*b*]fluoranthene were more susceptible to bioaccumulation in larval tissues over time. Overall, this study enhances our understanding of the impact of pollution on mosquitoes and could facilitate future research on the importance of symbiosis in urban-dwelling insect disease vectors. Given the recent advancements in the generation of axenic (microbe-free) and gnotobiotic (mosquitoes with a defined or specific microbiota) mosquitoes, further studies are needed to explore how changes in microbiota composition could influence mosquito responses to pollution, particularly in relation to host fitness, immunity, and vector competence.

## 1. Introduction

*Aedes* mosquitoes, such as *Aedes albopictus* and *Aedes aegypti,* are listed among the world's worst invasive alien species (Global Invasive Species Database, IUCN) (Lowe et al., 2004). These species are of critical public health importance as competent vectors for several infectious

* Corresponding author.
*E-mail address:* claire.valiente-moro@univ-lyon1.fr (C. Valiente Moro).
[1] Deceased

https://doi.org/10.1016/j.ecoenv.2024.117214
Received 15 July 2024; Received in revised form 7 October 2024; Accepted 16 October 2024
Available online 23 October 2024

diseases, including dengue fever, Zika virus, chikungunya, and yellow fever (Kraemer et al., 2019; Roiz et al., 2024). These diseases pose a significant threat to global health, particularly in tropical and subtropical regions, where *Aedes* mosquitoes are widespread (Guzman et al., 2010; Leta et al., 2018). The recent global expansion and redistribution of these mosquito species has increased the risk of arbovirus emergence in non-endemic areas (Medlock et al., 2015; Ryan et al., 2019). In particular, the Asian tiger mosquito, *Ae. albopictus,* has exhibited strong ecological plasticity, that allowed for its successful establishment in urban environments through adaption to various human-made habitats (Paupy et al., 2009; Bonizzoni et al., 2013; Dickens et al., 2018; Kolimenakis et al., 2021; Duval et al., 2023).

Meanwhile, urban environments are facing high levels of pollution due to rapid industrialization, population growth, and expanding infrastructure (Liang and Gong, 2020). The concentration of pollutants in these areas poses significant challenges for both environmental and public health (Manisalidis et al., 2020; Bikis, 2023). Among the most prevalent pollutants in urban settings are chemical contaminants such as heavy metals, polycyclic aromatic hydrocarbons (PAHs), and particulate matter, which are primarily generated by vehicle emissions, industrial activities, and waste management processes (Rhodes et al., 1983; Liu et al., 2019; Sun et al., 2021; Garagnon et al., 2023). These pollutants are persistent in the environment and can accumulate in air, water, and soil, leading to complex interactions that affect urban ecosystems. Therefore, aquatic and terrestrial organisms in these ecosystems are exposed to a constant influx of these substances, which can result in bioaccumulation and disrupt their physiology, behavior, and reproduction (Ali et al., 2019; Honda and Suzuki, 2020; Aziz et al., 2023). Most research papers have focused on PAH levels in air, soil, plants, or food matrices due to their carcinogenic properties and implications for food safety (Sampaio et al., 2021; Cui et al., 2022; Jesus et al., 2022). However, there remains a significant gap in our understanding of the specific mechanisms by which PAHs affect living organisms.

The study of insect exposure to environmental contaminants across various life stages has gained increasing attention due to critical roles of insects in pollination, decomposition, and food webs as well as their utility as sentinels for monitoring environmental pollution (Lambert et al., 2012). Insects with aquatic larval stages can accumulate contaminants like heavy metals and organic pollutants in their tissues (Hierlmeier et al., 2022). These contaminants are often retained through metamorphosis, affecting adult stages and potentially influencing insect survival, behavior, and reproduction (Bartrons et al., 2007; Kraus et al., 2014; Liu et al., 2018, 2020; Wesner et al., 2020). Moreover, exposure to pollutants also affects insect development, metabolism, and immune function, leading to altered growth rates, delayed development, and reduced reproductive success (Pölkki et al., 2012; Huang et al., 2020). Behavioral changes, such as impaired mating or flight, have also been observed, affecting population dynamics (Kozlov, 2022). However, some studies have shown little to no impact of environmental pollutants on some insect species (Straw et al., 2023; Ryalls et al., 2024). This means that some insects exhibit natural tolerance or have developed resistance mechanisms that allow them to survive and thrive in polluted environments. These adaptations may include efficient detoxification systems or changes in behavior that reduce exposure. Therefore, the impact of pollutants can vary widely between insect species from highly sensitive to highly tolerant species. Beyond impacting the host, pollutants can also influence their associated microbiota, as exemplified in many insect models (Antonelli et al., 2022). Changes in microbiota could then indirectly impact host physiology in either a beneficial (selection of taxa that might contribute to host tolerance) or deleterious way (pollutant-induced dysbiosis can enhance host susceptibility to pathogens) (Daisley et al., 2017).

Following previous observations, the ability of *Ae. albopictus* to thrive in polluted environments raise questions about their potential to bioaccumulate pollutants at various life stages and the subsequent impact on host physiology. Previous studies have shown contrasting effects of pollutants depending on the mosquito species, with some research showing negative impacts on development and survival, while other studies indicating minimal or no significant effects. In *Ae. aegypti*, PAHs induced cell mortality, detoxification process and oxidative stress, with effects varying depending on the PAH family member tested (Tetreau et al., 2014). In addition, PAHs modified the mosquito metabolism in a way that triggers its tolerance to insecticides (Poupardin et al., 2008). However, these results might not be generalizable, as the combined impact of UVs and Nitro-PAH (highly toxic derivatives of PAHs) induced susceptibility of *Cx quinquefasciatus* larvae to chemical insecticides (Ramkumar et al., 2022). In *Ae. albopictus*, heavy metals and microplastics were shown to alter their survival, reproduction and development (Ga'al et al., 2018; Yu et al., 2020; Zhou et al., 2020; Griffin et al., 2023). Apart from these studies focusing on the mosquito itself, no studies had yet investigated the impact of pollutants on mosquito-associated microbiota. However, the extent to which the microbiota is modified after exposure to pollutants throughout the mosquito life cycle, and the resulting effects on mosquito physiology-whether beneficial or deleterious- have not yet fully investigated. More research is needed on mosquito-specific responses to contaminants and the long-term effects of chronic exposure.

In addition to environmental pollutants in urban areas, the biological challenges posed by the Asian tiger mosquito are becoming an increasing concern. What remains unclear is the ability of this mosquito species to adapt to and withstand these pollutants, enabling its persistence in polluted environments. In this context, the aim of the present study was to investigate the level and extent of PAHs accumulation in both mosquito larvae and adults, as well as how PAHs exposure could affect mosquito-associated microbiota throughout their life cycle. We specifically address this question by focusing on PAHs due to their ubiquity in urban settings and their ecological impact on both living organisms and environmental microbial communities. More specifically, we investigated the following questions: (i) Does chronic exposure of *Ae. albopictus* to PAHs at realistic environmental concentrations affect the dynamics of mosquito-associated bacterial microbiota? (ii) what is the persistence and fate of these PAHs in water, particularly regarding their potential bioaccumulation in insect tissues?

## 2. Materials and methods

### 2.1. Establishment of indoor-mesocosms and sampling

Indoor-mesocosm experiments took place at Rovaltain Research Company (Valence, France). Two large ($4 \times 2\ m^2$) mesocosm chambers were built to mimic the natural habitats of *Ae. albopictus* mosquitoes (Fig. 1). Each mesocosm chamber contained identical features with a large stainless-steel basin (square of 120 cm side, depth 20 cm), vegetation with bamboo hedge and flowers as well as beakers filled with aged tap water and hay. Both pots and basins served as larval habitats, while bamboo hedge acted as mosquito resting sites. Mosquitoes had access to various potted plants (*Lobelia cardinalis, Iris versicolor, Veronica spicata, Ochagavia carnea, Cyperus alternifolius*) for nectar feeding and mosquito resting. Mice were made available to mosquitoes for blood feeding twice a week, for 2 hours each time, within each chamber. Mice were maintained in the animal house of Rovaltain Research Company agreed by direction départementale de la protection des populations, service Santé et Protection Animales (Departmental Directorate for the Protection of Populations, Health and Animal Protection Service, (agreement n° 2016336–0013) and used in accordance to European Union laws (directive 2010/63/UE). Throughout the experiment, mesocosms were maintained at a temperature ranging from 25 to 28°C, humidity level between 60 % and 80 %, a light intensity of approximately 800–1000 lux with a photoperiod cycle of 14/10 light/dark. *Ae. albopictus* mosquitoes used for experiments were insectary-reared (Pérols laboratory population from MIVEGEC laboratory, Montpellier, France) and maintained on a diet of rabbit hay, as previously described (Lacour et al., 2015). Each

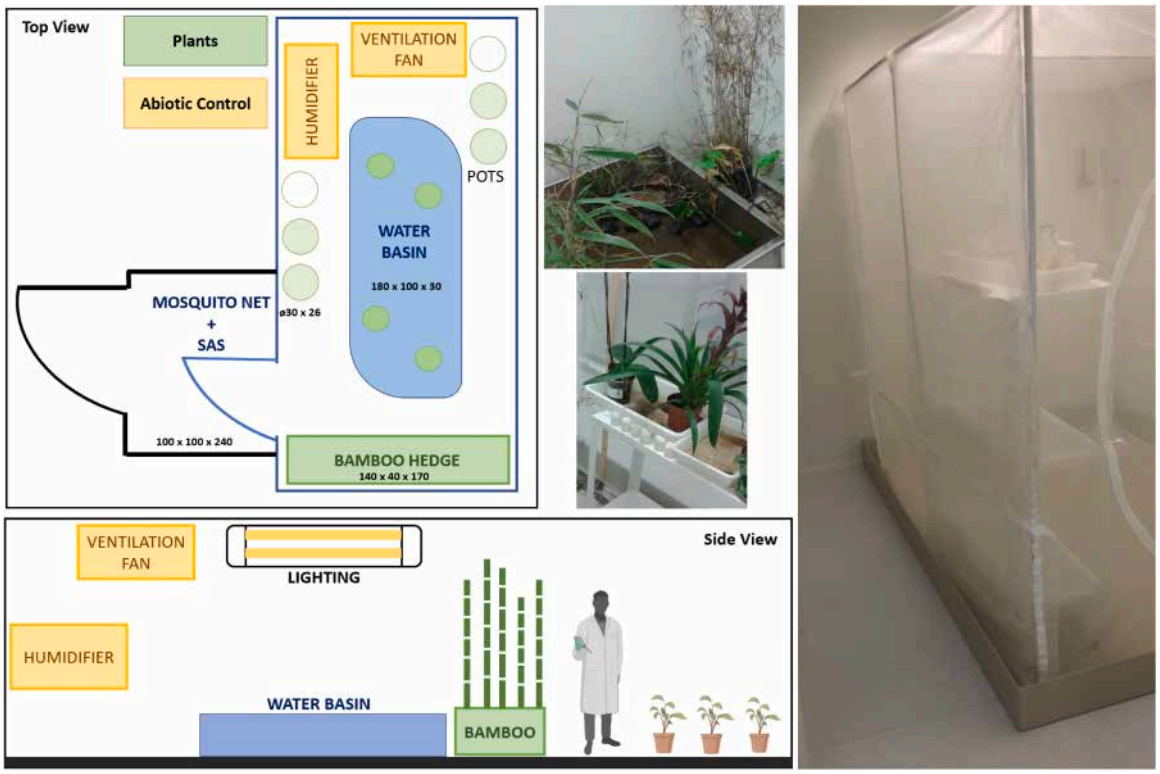


**Fig. 1. Design of indoor mesocosms for studying pollution exposure in *Ae. albopictus* populations.** The mesocosms comprise two large chambers (4 ×2 $m^2$) with identical features, including a large stainless-steel basin, vegetation with bamboo and flowers for larval habitats, nectar feeding and mosquito resting. Mice were made available to mosquitoes for blood feeding twice a week, for 2 hours each time. The mesocosm was maintained at a temperature ranging from 25 to 28°C, a humidity level between 60 % and 80 %, a light intensity of approximately 800–100 lux with a photoperiod cycle of 14/10 light/dark. Mesocosms were placed inside a rectangular shaped mosquito trap-net.

mesocosm was conditioned two weeks before the introduction of mosquitoes. At the beginning of the experiment, 100 *Ae. albopictus* L3-L4 larvae from the same colony batch were introduced in aquatic habitats to establish and synchronize *Ae. albopictus* populations in the two identical mesocosm chambers. Both mesocosms were placed inside a rectangular shaped mosquito trap net. One mesocosm was used as the control mesocosm while the second one was used as the treated mesocosm. The contaminated mesocosm was chronically treated with PAHs from the beginning of the experiment (day 0) and subsequently once a week by adding a cocktail of four PAHs at 2.5 µg/L each (Merck, Schnelldorf, Germany). PAHs generally occur in complex mixtures that can contain hundreds of compounds. We specifically focused on benzo[*a*]pyrene, benz[*a*]anthracene, chrysene and benzo[*b*]fluoranthene due to their environmental relevance, diversity of chemical structure and ecological impact (Lambert et al., 2012; Petrović et al., 2019). Samples were collected approximately 1, 2 and 3 months after the start of exposure in the treated mesocosm. For microbiota analysis, a random sampling of 20 males, 20 females and 20 larvae of three and fourth-instar larvae (L3/L4) was performed at 28, 63, 91 days from both mesocosms, along with triplicate 50 mL water samples from different larval habitats. Adult mosquitoes and larvae were collected using a mechanical aspirator and pipettes, respectively. Adult mosquitoes were sorted by sex and whole individuals (adults and larvae) were cold-anesthetized on ice, then surface-sterilized with absolute ethanol, as described by Zouache (Zouache et al., 2022). Afterwards, mosquitoes were dissected in sterile PBS using a stereomicroscope (10×) in a laminar flow hood to collect the gut. All samples were stored at −20°C until further use. For PAH bioaccumulation measurements, a random pool of 10 adults of each sex and 10 larvae (L3/L4) were collected in each mesocosm at 28, 56, 91 days post-exposure and stored at −20°C. Due to the limited number of individuals on day 56, it was not possible to synchronize sampling for microbiota and PAH bioaccumulation analyses at this time point. Water samples (50 mL) from both mesocosms were collected at 8, 22, 36, 45, 52, 62, 66, 80 and 86 days post population settlement (dpps) (n=5 per mesocosm*day) for PAH dosage.

### 2.2. Determination of PAHs concentration

PAH levels in mosquito tissues (larvae and adults) and water samples were measured as described by Pfannkoch *et al.* (Pfannkoch et al., 2015). Stir bar sorptive extraction (SBSE) was performed using GERSTEL Twister stir bars (PDMS 10 mm, 0.5 mm film thickness). Analysis was carried out on an Agilent 5890 Gas Chromatograph coupled with an Agilent 7000B Mass Spectrometer with a 70 eV electron impact source. For preparation, 10 adults or larvae were pooled and homogenized with 10 mL purified water using an Ultra Turrax homogenizer. Internal standards (BaP 13C4, Chrysene D12, and Naphtalene D8) were added directly to the tissue in the tube (0.002–1 mg/L concentration). Before QuEChERS extraction, samples were diluted with 10 mL of ACN and mixed for 1 minute. Then, 4 g of $MgSO_4$ and 1 g of NaCl were added, homogenized for 10 minutes on a GenoGrinder, and centrifuged at 4000 ×g for 5 minutes. For SBSE, 1.0 mL of the upper ACN layer was added to a 10 mL headspace vial containing a conditioned stir bar and 9 mL purified water and mixed for 60 minutes at 850 rpm. The stir bars were thermally desorbed into the GC at a flow rate of 100 mL/min, starting at 50°C and ramping to 290°C. Analytes were concentrated at −39°C and transferred to a column heated to 310°C with a 20:1 split ratio. Chromatographic separation was performed on an Agilent HP-5MS column (30 m x 250 µm x 0.25 µm) with helium at 1.2 mL/min. The column was held at 60°C for 0.5 minutes, then heated at 5 °C/min to 320°C and held for 3 minutes, totaling 55.5 minutes. Detection was done using multiple reaction monitoring (MRM) mode. Detection was simultaneously

carried out using multiple reaction monitoring (MRM) mode.

### 2.3. DNA extraction, library preparation and sequencing

Water samples (22 mL aliquot) were centrifuged following the method described by Zouache et al. (2022). Gut samples were individually crushed with 1-mm diameter beads in ATL lysis buffer (Qiagen, Hilden, Germany) containing 20 mg/mL lysozyme (Euromedex, Strasbourg, France) using a Mini-BeadBeaterTP apparatus (BioSpec Products, Bartlesville, USA). DNA from both water and gut samples was subsequently extracted in 18 batches using the Qiagen DNeasy Blood and Tissue kit (Qiagen, Roermond, Germany), as previously described (Minard et al., 2015). A negative control (no biological matrix) was included in each batch. Amplicon sequencing of bacterial communities was performed as previously described in Zouache et al. (2022). PCR products were purified using the Agencourt AMPure XP PCR Purification kit (Beckman Coulter, Paris, France) and quantified using the Quant-iT Picogreen dsDNA Assay Kit (Life Technologies, Carlsbad, USA) (Table S1). Sequencing of the PCR libraries was conducted on Illumina MiSeq platforms with a v3 cycle kit at Biofidal (Vaulx-en-Velin, France). All FastQ files have been deposited in the EMBL European Nucleotide Archive (https://www.ebi.ac.uk/ena) under the project accession number PRJEB77294.

### 2.4. Bioinformatics analysis

A total of 17,593,725 reads were generated from 16S rRNA high-throughput sequencing. Pair reads were merged using PEAR (ver. 0.9.8) with default parameters. Quality control and clustering into amplicon sequences variants (ASVs) were performed using the FROGS pipeline (Escudié et al., 2018). Briefly, denoising was carried out by discarding reads out of the expected targeted sequence range (250–350 bp range). Then, clustering was performed using the SWARM algorithm based on an aggregation distance of 1 in order to generate the ASVs (Bernard et al., 2021). Chimera were discarded using VSEARCH (Rognes et al., 2016) and low frequency ASVs (<0.005 %) were also filtered out (Bokulich et al., 2013). Taxonomic annotation of ASVs was conducted following their alignment using the Mothur pipeline and identification based on the Silva v138.1 database, with an alignment cutoff settled to 80 % (Quast et al., 2013). From this step, data were separated into three tables corresponding to (i) the whole dataset (Water, Larvae, Adults), (ii) the water dataset and (iii) the insect dataset (Larvae, Adults). Such split allowed normalization with a higher number of reads and a better comparison within the sample type (Water, Larvae and Adults). ASVs within samples were corrected using negative controls (blank extraction and PCR) to remove ASVs if their relative abundance was not at least 10 times higher than that observed in the negative controls (Minard et al., 2015). Normalization for sample comparison and analysis was performed by randomly resampling down to 152, 676 and 396 sequences (*i.e.* lower number of reads in sample for each dataset) in the whole dataset, the water dataset and the insect dataset, respectively. Correlations between the 50 most abundant ASVs were calculated using the Spearman correlation coefficient for the insect dataset and used to create an ASV network for each mesocosm. Only positive correlations, greater than 0.3, were kept and highlighted between ASVs in a network created using GEPHI software and Fruchterman-Reingold algorithm (Fruchterman and Reingold, 1991; Bastian et al., 2009). ASV sizes were proportional to the abundance of each ASV.

### 2.5. Diversity and statistical analysis

Data analysis and statistical tests were carried out using R Statistical Software (v4.2.2, R Core Team, 2022) using the *vegan* package for diversity analysis (Oksanen et al., 2015) as well as the *ggplot2* (Wickham, 2016) and *ComplexHeatmap* packages (Gu, 2022) for graphical representations. The ASVs that represent at least 12 % of total abundance in at least one sample were selected to generate a heatmap showing the ASV abundance variations across insect stage and collection time point. Graphical diagrams of average bacterial composition within each condition (treatment, sample type) at different taxonomic levels (family, order) were obtained using *phyloseq* package (McMurdie and Holmes, 2013). Within-sample diversity (*i.e.* α-diversity) was estimated through the Shannon-Weaver index. Then, linear models were performed with square transformed Shannon diversity index as the response variable and, time and sample (water, larvae, adult) as explanatory variables. For adults, a second model was carried out by using square transformed Shannon diversity index as the response variable and, time and sex as explanatory variables. Contribution of those explanatory variables on variability of the Shannon index were tested with an analysis of variance (ANOVA) and a Tukey *post-hoc* test using the *car* (Fox and Weisberg, 2019) and *emmeans* (Lenth, 2023) R packages. The residuals of the model were verified for normality and homoscedasticity using the *DHarma* package (Hartig, 2022). Bacterial communities' dissimilarities among samples (*i.e.* ß-diversity) were represented using the Bray-Curtis index in a non-metric multidimensional scaling (NMDS). Subsequent analyses of the ß-diversity were performed using permutational multivariate analysis (*vegan* package). Distance-based redundancy analyses (dbRDA) were used to constrain separation between samples according to sample categories, treatment, time and sex to determine the most discriminant ASVs responsible for the observed differences between bacterial communities. Homogeneity of the communities (*i.e.* ß dispersion) within the sample type (waters, larvae and adults) for both mesocosm over time was tested through permutational analysis. PAHs concentrations in mesocosms overtime were compared with a linear model with PAHs concentrations used as a response variable and treatment and time used as explanatory variables. Model parameters were tested with an ANOVA followed by a Tukey *post-hoc* test.

## 3. Results

### 3.1. Indoor-mesocosm experiments are relevant facilities for studying the dynamics of mosquito bacterial assemblages across developmental stages

Two independent populations of *Ae. albopictus* were established within indoor-mesocosms reflecting environmental parameters. Following the initial introduction of mosquitoes, *Ae. albopictus* populations successfully thrived and reproduced, as evidenced by the continuous production of eggs, larvae and adults throughout the observation period (3 months). From the 409 total samples collected in both control and treated mesocosms, analysis of bacterial communities associated with mosquitoes and their breeding waters enabled the identification of 1504 bacterial ASVs, distributed among 5 phyla and 52 genera (including one unclassified). In the control mesocosm, the α-diversity (species richness) significantly differed over time (ANOVA: $F=9.45$, $df = 2$, $p\text{-value}=0.0001$), between sample types (water, larvae, adults) (ANOVA: $F=42.25$, $df=2$, $p\text{-value}= 6.8\text{x}10^{-16}$) and their interaction (ANOVA, $F=3.21$, $df=4$, $p\text{-value}=0.013$) (Fig. 2**A**). Overall, adults harbored a more diverse bacterial microbiota compared to larvae and their water habitat at 28 dpps (Tukey-HSD, $p\text{-values} < 0.0002$), as well as compared to water habitats but only at 91 dpps (Tukey-HSD, $p\text{-value} = 0.0087$). This trend was not statistically significant at 63 dpps (Tukey-HSD, $p\text{-value} > 0.05$). There were no significant differences in α-diversity according to the sex of mosquitoes at any time point and overall (ANOVA, $F=0.45$, $df=1$, $p\text{-value} = 0.50$) (Figure S1). On average, 22.50, 40.04, and 65.64 ASVs were found throughout the entire experimental period in water, larvae, and adult samples, respectively. Almost two thirds (61.3 %) of ASVs detected in water samples were also found in larvae and 32.3 % of those observed in larvae were also detected in adults (Fig. 2**B**). ß-diversity analyses revealed that different sample types harbor divergent bacterial communities (PERMANOVA, $R^2=0.148$, $p\text{-value}<0.001$) (Fig. 2**C**). This community also differed over time, albeit to

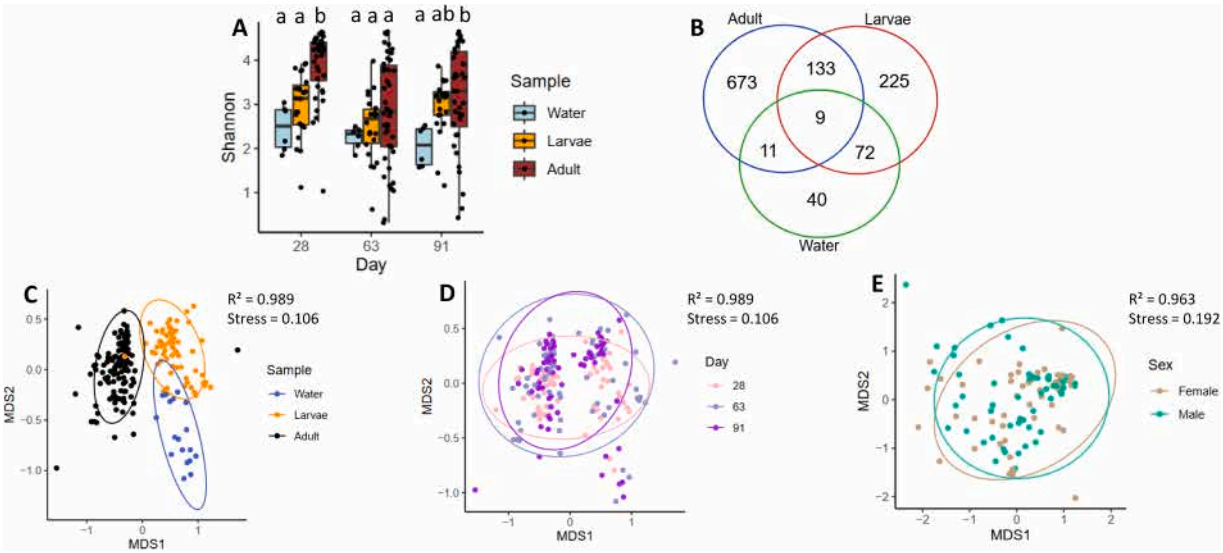


**Fig. 2. Comparison of diversity metrics of bacterial communities in mosquitoes and their breeding sites. (A)** Boxplots of alpha diversity values distribution for Shannon diversity index based on variance in species evenness, are represented for each sample type (water, blue; larvae, orange; adults, dark red) over time. Significance between sample types and time was determined using analysis of variance (ANOVA) based on a linear model. Boxplots with different letters indicate significant differences based on post-hoc tests used to compare sample types at each collection time point. **(B)** Venn diagram showing ASVs shared across sample types. **(C - E)** Beta-diversity based on Bray-Curtis distances visualized in an NMDS plot. NMDS plots show the differences in the bacterial community composition of the DNA samples. Data were grouped and plotted according to sample type **(C),** time **(D),** and adult sex **(E)**. Ellipses are drawn to represent the 95 % confidence regions for group clusters.

a lesser extent (PERMANOVA, $R^2$=0.028, *p-value*<0.001) while this longitudinal deviation was heterogeneous according to each sample type (PERMANOVA: $R^2$=0.054, *p-value*<0.001) (Fig. 2**D**). In contrast, the composition of the microbiota seemed to be similar between sexes (PERMANOVA, $R^2$=0.005, *p-value*=0.929) (Fig. 2**E**). The homogeneity of bacterial communities was then assessed over time for each sample type. Bacterial communities associated with larvae were significantly more homogeneous over time (permutation test, *p-value* =0.003) (Figure S2A). Notably, bacterial communities were more uniform at 91 dpps compared to 63 dpps (permutation test, *p-value*=0.001). Adults (permutation test, *p-value*=0.883) and water samples (permutation test, *p-value*=0.407) did not show any significant differences in the homogeneity of their microbiota over time (Figure S2B and S2C). Proteobacteria was the major phylum in each sample type (Figure S3A). Analysis between the microbiota of adults and larvae highlighted that ASVs identified as members of the Comamonadaceae family were more abundant in larvae, while ASVs identified as belonging to Anaplasmataceae, Acetobacteraceae and Enterobacteriaceae family were mostly associated with the adult microbiota (Figure S3B; Table S2). The microbiota shift between adults and larvae highlighted that ASVs identified as belonging to Comamonadaceae and Enterobacterales were mostly associated with larvae, while *Wolbachia*, *Asaia* and *Klebsiella* were rather associated with adult mosquitoes, with *Klebsiella* being specifically associated to adults (Fig. 3). Network analysis based on co-occurrences of the 50 most abundant ASVs highlighted that the bacterial community was structured according to the insect stage, with two distinct clusters: one corresponding to ASVs associated with larvae and the other with adults (Figure S4A). Larvae microbiota was structured with ASVs belonging to Comamonadaceae family while adult microbiota was structured around two major ASVs identified as *Wolbachia* and *Asaia*, which respectively dominated the two subsgroups within the adult cluster (Figure S4A). Over the course of the experiment, the proportion of Enterobacterales spp and *Lacihabitans* in larvae decreased in favor of Comamondaceae spp (Table S2). In adults *Wolbachia* progressively replaced *Cedecea*, *Asaia* and *Ralstonia* (Table S2). For water samples, ASVs identified as Chitinophagaceae spp, *Arenimonas*, and *Aurantimicrobium* were mostly associated with the water breeding sites (Table S2).

### 3.2. *Fate of PAHs in mesocosms colonized by mosquitoes and their impact on the dynamics of bacterial assemblages*

To evaluate how environmental exposure to PAHs impacts on bacterial communities in mosquitoes and their breeding sites, aquatic habitats of the treated mesocosm were contaminated with a cocktail of four PAHs (chrysene, benz[*a*]anthracene, benzo[*a*]pyrene and benzo[*b*] fluoranthene). At 8 dpps, the treated mesocosm exhibited 7.2 times higher PAHs concentrations than the control mesocosm (ANOVA, F=10.62, df=1, p-value=0.001). These higher concentrations persisted during the first 45 days (Tukey-HSD, before day 45, p-values<0.005) (Fig. 4**A**). From day 52, PAH concentrations in the treated mesocosm lowered to basal concentrations of the control mesocosm (Tukey-HSD, after day 45, *p-values*>0.005). The four PAHs were detected in all samples except in adults at 28 dpps, with total PAHs concentrations ranging from 7.340 to 29.490 ng/10 mosquitoes (Fig. 4**B**). Exposed larvae exhibited PAHs concentrations twice as high as their untreated counterparts at each collection time point, with a linear increase in total PAHs bioaccumulation overtime ranging from 1.549 ng/larvae at 28 dpps to 2.949 ng /larvae at 91 dpps. Meanwhile, adults from the treated mesocosm accumulated only 19 % more PAHs than their untreated counterparts (Fig. 4**B**). More specifically, benzo[*b*]fluoranthene and benzo[*a*]pyrene were the most bioaccumulated PAHs in larvae, reaching respectively concentrations 3.28 and 2.52 times higher than the basal concentrations detected in larvae of the control mesocosm (Fig. 4**C**). In the treated mesocosm, a total of 1089 ASVs were detected. Alpha-diversity in this mesocosm was mainly influenced by the sample type (ANOVA, F=24.31, df = 2, *p-value*=$5x10^{-10}$) and collection time point (ANOVA, F=3.56, df = 2, *p-value*=0.03), but not their interaction (ANOVA, F=1.5446, df=4, *p-value*=0.19) (Fig. 5**A**). *Post-hoc* analyses revealed that adults had more diverse bacterial communities than water samples (Tukey-HSD, *p-value* = 0.0011) and larvae (Tukey-HSD, *p-value* = 0.0011) at 28 dpps, and compared to larvae at 91 dpps (Tukey-HSD, *p-value* < 0.0001) (Fig. 5**A**). Collection time point also impacted the α-diversity of adults, as it decreased after the first sampling at 28 dpps

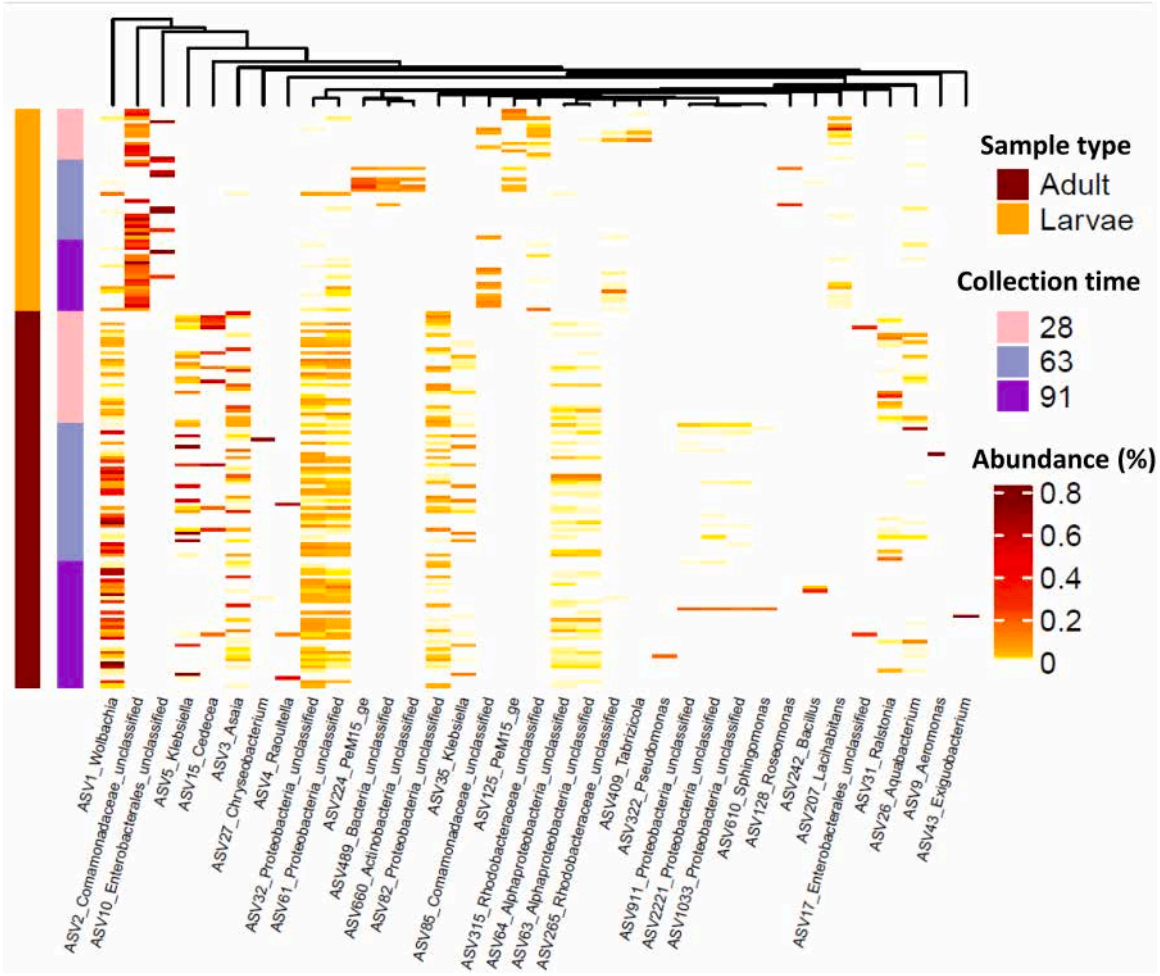


**Fig. 3. Heatmap showing the relative abondance of the mosquito-associated bacterial composition in larvae and adult samples**. Bacterial ASVs that represent at least 10 % of the total bacterial abundance in at least one sample are represented in columns. ASVs are grouped according to the result of hierarchical clustering based on the Euclidean dissimilarity distance. Each sample is shown on the *Y*-axis and is representing with a color code (larvae, orange; adults, dark red) for each collection time point (28, pink; 63, blue; 91, purple). Heatmap colors (from white to dark red) indicate increasing abundance of each bacterial microbiota component.

(28–63 comparison, Tukey-HSD, *p-value* = 0.0059; 28–91 comparison, Tukey-HSD, *p-value* = 0.0272) **(**Fig. 5**A)**. Moreover at 28 dpps, males exhibited higher α-diversity than females (Tukey-HSD, *p-value* = 0.0413) **(**Figure S1**)**. On average, 22.00, 31.13, and 66.86 ASVs were identified throughout the entire experiment in water, larvae and adult samples, respectively. Only 34.4 % of the ASVs detected in water were detected in larvae, and 42.6 % of those observed in larvae were also detected in adults (Fig. 5**B**). ß-diversity analyses indicated that bacterial communities in this mesocosm were largely shaped by the sample type (PERMANOVA, $R^2$=0.15, *p-value*<0.001), the day post population settlement (PERMANOVA, $R^2$=0.03, *p-value*<0.001), and to a lesser extent by their interaction (PERMANOVA, $R^2$=0.06, *p-value*<0.001) (Figs. 5**C and** 5**D**). Contrary to what was observed in the control mesocosm, the sex of mosquitoes had a small but significant effect on bacterial communities, accounting for 2 % of the observed differences (PERMANOVA, $R^2$=0.02, *p-value* = 0.021) (Fig. 5**E**). Similarly to observations made in the control mesocosm, the bacterial communities associated with larvae tended to become more homogenous overtime (permutation-test, *p-value* =0.06), particularly in the latest sampling periods collected (28–91 comparison, permutation-test, *p-value*=0.04) **(**Figure S2D**)**. On the contrary, water bacterial community compositions were more divergent over time (permutation-test, *p-value* = 0.028) while that of adults did not change (permutation-test, *p-value* = 0.875) **(**Figure S2E and S2F**)**. At the taxonomic level, ASVs identified as Comamonadaceae, Rhizobiaceae and Gammaproteobacteria were mostly associated with larvae **(**Table S3**)**. Notably ASVs identified as members of the Comamonadaceae family were the most abundant throughout the course of the experiment, while ASVs identified as members of the Rhizobiaceae family decreased over time **(**Table S3**)**. ASVs assigned as *Wolbachia*, *Asaia* and *Raoultella* were mainly associated with adults, with some specificities according to the sex of mosquitoes **(**Table S3**)**. For instance, some microbiota members such as Enterobacterales and *Cedecea* were enriched in females, while *Wolbachia* and *Raoultella* were rather enriched in males **(**Table S3**)**. Over the course of the experiment, ASVs associated to Enterobacterales spp, *Ralstonia* and *Cedecea* decreased while *Asaia*, *Wolbachia*, *Raoultella* and *Aeromonas* increased **(**Table S3**)**. Over the course of the experiment, ASVs associated to Enterobacterales spp, *Ralstonia* and *Cedecea* decreased while *Asaia*, *Wolbachia*, *Raoultella* and *Aeromonas* increased **(**Table S3**)**. Similar to the control mesocosm, the bacterial community was structured according to the insect stage, forming two distinct clusters: the first associated with larvae, dominated by Comamonadaceae spp, and the second associated with adults, which was divided into two subgroups, each dominated by *Wolbachia* and *Asaia*, respectively **(**Figure S4B**)**. Interestingly, another cluster linked to the adult cluster, composed of *Klebsiella*, *Aeromonas* and *Cedecea* was also identified **(**Figure S4B**)**. Finally, Sporichthyaceae and bacteria belonging to *Variovorax* and *Limnobacter* genera were mainly associated with water samples **(**Table S3**)**.

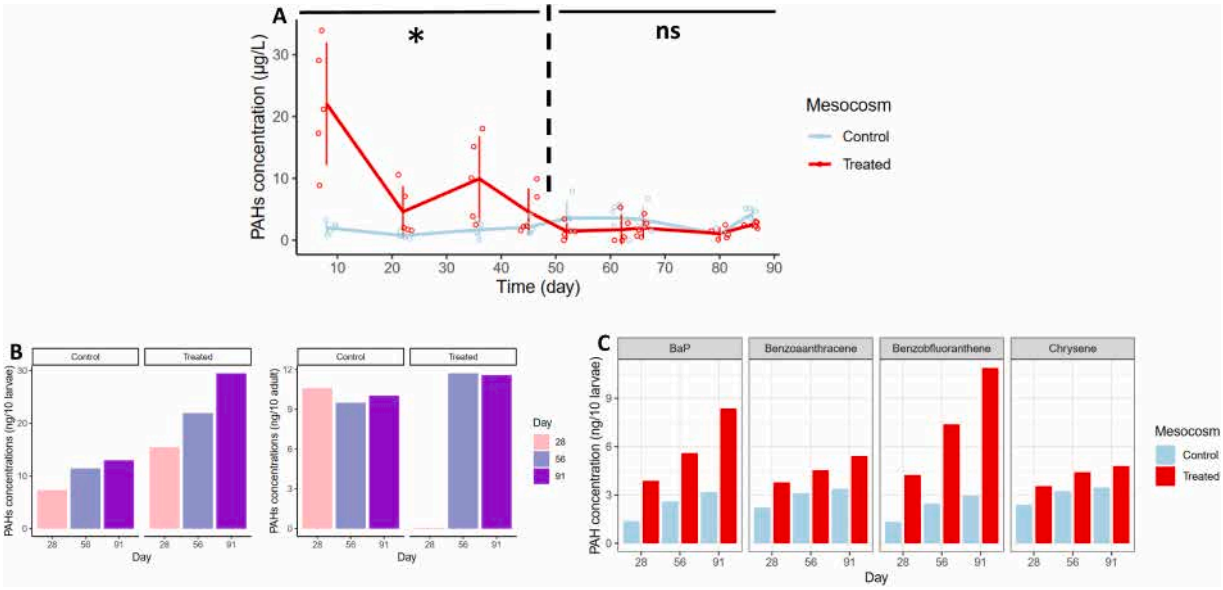


**Fig. 4. Fate of PAHs in mesocosms and bioaccumulation within mosquito tissues. (A)** Mean concentrations of PAHs in water samples (n=5, for each collection time point) and standard deviations are represented (blue, control mesocosm; red, treated mesocosm). Significant differences in PAHs concentration between mesocosms were determined using analysis of the variance (ANOVA) based on a linear model and post-hoc complementary analysis for each day comparison (*: *p-value*<0.05; ns: p-*value*>0.05). **(B)** Barplots showing PAHs concentrations within pools of 10 larvae or adults over time in the control and treated mesocosms for each collection time point (28, pink; 63, blue; 91, purple). **(C)** Barplots showing the bioaccumulation of each PAH within larval tissues over time (blue, control mesocosm; red, treated mesocosm).

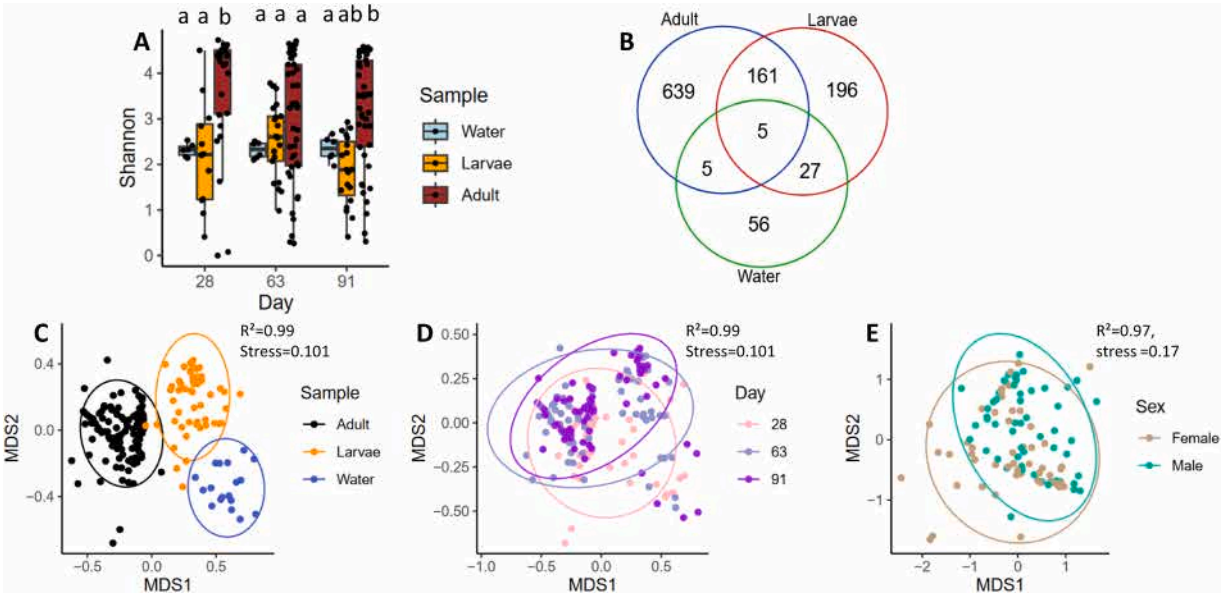


**Fig. 5. Comparison of diversity metrics of bacterial communities in mosquitoes and their breeding sites in a HAPs polluted context. (A)** Boxplots of alpha diversity values for Shannon diversity index based on variance in species evenness, are represented for each sample type (water, blue; larvae, orange; adults, dark red) over time. Significance between sample types and time was determined using analysis of variance (ANOVA) based on a linear model. Boxplots with different letters indicate significant differences based on post-hoc tests used to compare sample types at each collection time point. **(B)** Venn diagram showing ASVs shared across sample types. **(C - E)** Beta-diversity based on Bray-Curtis distances visualized in an NMDS plot. NMDS plots show the differences in the bacterial community composition of the DNA samples. Data were grouped and plotted according to sample type **(C),** time **(D)** and adult sex **(E).** Ellipses are drawn to represent the 95 % confidence regions for group clusters.

### *3.3. The presence of PAHs led to the modification of major taxa in mosquito microbiota*

The impact of PAHs on bacterial communities associated with mosquitoes and their water breeding sites was also assessed through inter-mesocosm analysis. PAHs did not significantly impact the α-diversity of bacterial communities associated with water samples (Kruskal, *p-value* = 0.29) or adults (ANOVA, F=0.63, df=1, *p-value* = 0.42) (Figure S1). However, they modified the α-diversity of larvae (ANOVA, F=8.07, df=1, *p-value*=0.005), especially at 91 dpps (Tukey-HSD, *p-value* = 0.0001) (Figure S1). In addition, PAHs influenced the composition of water bacterial communities over time (PERMANOVA, $R^2$ = 0.286, *p-values*<0.001). *Arenimonas*, Chitinophagaceae, and *Aurantimicrobium* were mainly associated with water samples from the

control mesocosm while Sporichthyaceae and *Variovorax* were rather associated with the treated one (Table S4). The bacterial composition of larvae differed over time between treated and control mesocosms (PERMANOVA, $R^2$=0.12, *p-values*<0.001) (Figs. 6**A and** 6**C**). Separate analyses indicated that PAHs-induced changes were of similar magnitude overtime for each day, showing a shift of 12.6 %, 12.3 % and 12.6 % of the bacterial community at 28, 63 and 91 dpps, respectively (Figure S5). Overall, unclassified Enterobacterales and two unclassified Gammaproteobacteria were specific to larvae from the control mesocosm while two Comamonadaceae spp, Rhizobiaceae and a Gammaproteobacteria were rather associated to larvae from the treated mesocosm (Table S4). Over the course of the experiment, ASVs that increased or decreased in one mesocosm had the same trend in the second mesocosm (Table S4). Finally, bacterial communities associated with adults were also influenced by PAHs and varied over time, albeit to a lesser extent than those associated with larvae (PERMANOVA, $R^2$=0.065, *p-values*<0.001) (Figs. 6**B and** 6**D**). At 28, 63 and 91 dpps, PAHs exposure induced a shift in the bacterial community composition (Figure S5). PAHs were responsible for 4 %, 8 % and 1.6 % of the observed differences, respectively, with shifts being significant at 28 and 63 dpps (PERMANOVA, *p-values*<0.001) (Figure S5). *Wolbachia*, *Klebsiella*, and *Cedecea* were rather associated to adults from the control mesocosm while *Asaia*, *Raoultella*, an unclassified Enterobacterales and *Aeromonas* were enriched in adults from the treated mescosm (Figure S4A and S4B; Table S4). In both mesocosms, *Wolbachia* and *Raoultella* proportions increased over time while that of *Ralstonia* and *Cedecea* decreased (Table S4). Interestingly, *Asaia* proportion decreased in the control mesocosm while its proportion increased in the PAHs-treated mesocosm (Table S4).

## 4. Discussion

Mesocosm-based experiments constitute a valuable approach to explore the impacts of environmental stressors on species at population level and over several generations (Lawton, 1996). However, the use of mesocosms mimicking the natural habitat of mosquitoes is still scarce (Ng'habi et al., 2018; Choo et al., 2021; Olkeba et al., 2021; Dellar et al., 2022). In the present study, *Ae. albopictus* populations were maintained in indoor mesocosms, with one remaining untreated, and the other polluted with PAHs. This approach allowed for the characterization of the dynamics of mosquito-associated bacterial microbiota over 3 months in the presence or absence of a cocktail of PAHs, as well as monitoring the detection of PAHs within the mesocosms.

One of the most striking results was the observed drop in PAHs concentrations in the treated mesocosm after 45 days reaching basal levels of the control mesocosm. Such a decrease could be explained either by the presence of PAH-degrading bacteria (Peng et al., 2008; Baldantoni et al., 2017;Patel et al., 2020), or the accumulation of PAHs within the sediments due to their hydrophobic nature, rendering them less accessible for biological uptake or detection (Hussain et al., 2018; Jesus et al., 2022), or by the bioaccumulation in animal tissues as already observed for bees, urchins or in dragonfly nymphs (Perugini et al., 2009; Girardin et al., 2020; Albarano et al., 2021). Without excluding the first two hypotheses, we demonstrated that PAHs bioaccumulate within tissues of larvae originating from the breeding sites of the treated mesocosm. Interestingly, only benzo[*a*]pyrene and benzo[*b*]fluoranthene out of the four PAHs were detected at higher concentrations in larval tissues compare to larvae from the control mesocosm. Benzo[*b*]fluoranthene has already been identified as a PAH capable of bioaccumulating in bees, whereas benzo[*a*]pyrene was never detected (Perugini et al., 2009). Additionally, bees were found to bioaccumulate benz[*a*]anthracene, though in our study, this compound was not bioaccumulated in larval tissues (Perugini et al., 2009). These findings support that PAHs bioaccumulation may vary depending on the contamination source and the insect species involved. Contrary to larvae, PAHs were not bioaccumulated in adult mosquito tissues suggesting their potential elimination during metamorphosis. The detection of PAHs and metals only in the immature stages of insects has already

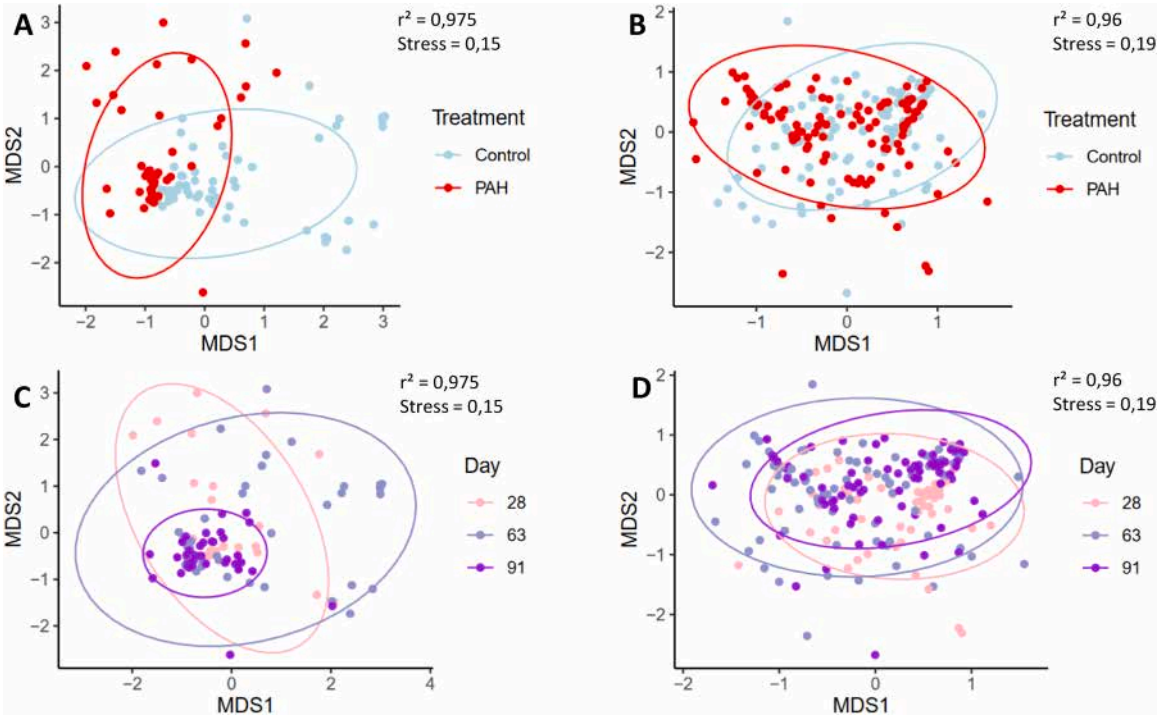


**Fig. 6. Dynamics of PAHs impact on bacterial communities in larvae and adult mosquitoes.** Beta-diversity based on Bray-Curtis distances visualized in an NMDS plot. NMDS plots show the differences in the bacterial community composition of the DNA samples. For larvae, data were grouped and plotted according to PAH presence **(A)** and collection time point **(C)**. Similarly, for adults, data were also grouped and plotted according to PAH presence **(B)** and time **(D)**. Ellipses are drawn to represent the 95 % confidence regions for group clusters.

been reported (Kraus et al., 2014). This could be explained by variations in exposure throughout the insect's life cycle. While mosquito larvae are continuously exposed throughout their development in water and can acquire PAHs through ingestion or contact, adults might only be exposed to polluted waters during egg-laying, emergence or drinking. It is also possible that PAHs could be excreted and/or metabolized during immature life stages as previously observed for metals in living organisms (Aoki and Suzuki, 1984; Hare, 1992; Luoma and Rainbow, 2005). However, this phenomenon might depend on the pollutant and/or the insect species, as microplastics, polychlorinated biphenyl or certain pesticides have been reported throughout the insect lifecycle (Kraus et al., 2014; Al-Jaibachi et al., 2019). Finally, the absence of PAHs detection in adults could be due to survivor bias. In addition to storing lipids needed for overcoming metamorphosis, fat body is also used as a storage site for pollutants (Jackson et al., 2017). Fat body shrinking resulting from energy consumption over metamorphosis could lead to an acute release of pollutants lethally intoxicating individuals.

Our results showed that PAHs induce variations in the composition and diversity of bacterial communities associated with adults and larvae, as previously described in mouse or fish models (Ribière et al., 2016; Xie et al., 2020). The observed decrease in α-diversity is associated with an increase in PAHs bioaccumulation within larvae, suggesting a potential relationship. Previous studies in other biological models have already demonstrated that elevated levels of PAHs can disrupt microbial community structure, leading to reduced diversity (Zhao et al., 2019; Xie et al., 2020; Zhang et al., 2021). According to our study, the developmental stage appeared to play a significant role in the restructuring of bacterial communities in the presence of PAHs, particularly in larvae. The differential impact of PAHs between larvae and adults may result from lower bioaccumulation in adults or differences in biological life stages. ASVs belonging to the Comamonadaceae family that structured the larvae microbiota, showed significant enrichment (19.4 % *vs* 30.4 % of the whole sequences) in larvae reared in the PAH-treated mesocosm. Members of this family are commonly found in the gut and cuticular microbiota of mosquito species (David et al., 2016; Dada et al., 2021; Caragata et al., 2022; Trzebny et al., 2023). This enrichment could be due to positive selection resulting from their potential ability to degrade PAHs *via* dioxygenases activities (Moser and Stahl, 2001) and/or negative selection of the remaining microbiota. Furthermore, the genus *Comamonas* has been demonstrated to contribute to the development and fecundity of *Aedes atropalpus* (Coon et al., 2016). This association could be favored if certain members of Comamonadaceae can degrade PAHs within larvae. Thus, the bacterium is potentially contributing to host detoxication activities while benefiting as carbon nutrition for themselves. Larvae not exposed to PAHs were also associated with unclassified Enterobacterales (11 % *vs* 0 %) and other taxa such as *Lacihabitans* (1.3 % *vs* 0 %) and Gammaproteobacteria spp (2.1 % *vs* 0 %) which are commonly associated with aquatic organisms (Xie et al., 2021; van der Loos et al., 2023). This suggests that Comamonadaceae, which are predominantly present in larval microbiota in the absence of PAHs exposure, appear to be favored by the presence of PAHs. Previously, amplification of taxa with large genomes, such as Comamonadaceae (Biessy et al., 2022; Hem et al., 2022) had been observed in the presence of PAHs (Dong et al., 2022). These authors showed that PAH selection pressure resulted in the selection of organisms with larger genomes, enhancing their adaptability and the microbial community's ability to communicate, notably through horizontal gene transfer.

For bacterial communities associated with adults, the overall impact of PAH varied over time and was less pronounced than in larvae. Since it was not possible to ensure age consistency for the adult collection in both mesocosms, we cannot exclude that differences observed in microbiota composition may be also attributed to age-related variations in mosquitoes, as they can live for up to one month in an indoor facility (Cui et al., 2021). However, to our knowledge, no studies have yet investigated the dynamics of mosquito-associated microbiota throughout their adult life span. Under PAHs exposure, specific ASVs such as *Asaia* (3.8 % *vs* 12.4 %), *Raoultella* (1.2 % *vs* 5.6 %) and *Aeromonas* (0 % *vs* 1.9 %) were found to be enriched, while others ASVs like *Wolbachia* (12.8 % *vs* 6.5 %), *Klebsiella* (5.6 % *vs* 0.6 %) and *Cedecea* (3.7 % vs 0.8 %) were depleted. Furthermore, these differences were not influenced by the sex of mosquitoes. *Raoultella* and *Aeromonas* are known to degrade PAHs in soil and aquatic ecosystems, but their ability to perform these activities in insects has not yet been demonstrated (Alegbeleye et al., 2017; Ping et al., 2017; Agrawal et al., 2019). *Aeromonas* dominates the microbiota of mosquito populations exhibiting high resistance to the temephos insecticide (Soltani et al., 2017), indicating that this bacterium likely possesses detoxication capabilities. Moreover, in the mosquito species *Culex pipiens*, *Aeromonas* may act as an attractant for oviposition habitat selection and contribute to larval molting (Díaz-Nieto, 2016). However, these bacteria have also been reported to opportunistically infect fish and crustaceans (Noonin et al., 2010; Chaix et al., 2017; Dubey et al., 2022). In the rainbow trout *Oncorhynchus mykiss*, long-term exposure to PAHs increased susceptibility to *Aeromonas* (Bravo et al., 2011) by altering its immune system (Curtis et al., 2017). Therefore, we could hypothesize that the enrichment of *Aeromonas* in the treated mesocosm could be a result of indirect alteration of the mosquito immune system. However, the presence of *Aeromonas* could also be due to its selection within the host if the bacterium is tolerant and capable of metabolizing PAHs *in insecta*. *Asaia* (the third enriched ASV in adults) is not known to degrade PAHs but has been found to degrade other compounds, such as the pyrethroid insecticide, as revealed by comparative genomic studies in mosquitoes (Comandatore et al., 2021). Conversely, an overabundance of *Asaia* has also been observed in *Anopheles coluzzii* populations susceptible to deltamethrin, a pyrethroid insecticide (Pelloquin et al., 2021). Similarly, *Asaia* was found in higher abundance in *Anopheles gambiae* mosquitoes exposed to glyphosate herbicide, which increased their permissiveness to *Plasmodium,* the human malaria parasite (Smith et al., 2021). This phenotype might be the result of a more complex system than just the presence of *Asaia*, as *Asaia* has also been shown to elicit an anti-plasmodium response in *Anopheles stephensi* (Cappelli et al., 2019). Taken together, these observations suggest that *Asaia* could serve as a microbial marker for mosquitoes exposed to various environmental stressors. The three ASVs that were less abundant in the midguts of adult mosquitoes exposed to PAHs (*Wolbachia*, *Klebsiella* and *Cedeceae*) belong to genera commonly found in insects. These genera were shown to be involved in various insect functions such as reproduction, development, detoxification or immunity (Kyritsis et al., 2017; Mariño et al., 2017; Yin et al., 2023). Their absence could indicate a dysbiosis that significantly disrupt host functions. Indeed, *Wolbachia* and *Cedecea* are known to influence the structure of the insect microbiota, particularly by excluding specific taxa such as the opportunistic entomopathogen *Serratia marcescens* (Kozlova et al., 2021). Moreover, *Cedecea* is involved in biofilm formation, thereby favoring in the gut colonization by microbial symbionts (Hegde et al., 2019). Therefore, we could hypothesize that PAHs disrupt the ability of *Cedecea* to modulate microbiota and exclude pathogens. Additionally, *Wolbachia* not only modulates bacterial microbiota but also exhibits antiviral effects across different kingdoms (Johnson, 2015). *Wolbachia* exploits mosquito innate immunity, thereby influencing vector competence. Moreover, *Cedecea* and *Wolbachia* may have been depleted despite their detoxication capabilities against anthropogenic stressors such as antibiotics, insecticides and herbicides (Brennan et al., 2008; Thompson and Sharkady, 2020; Algamdi et al., 2023; Ma et al., 2023), possibly in favor of specific PAH-degrading taxa like *Raoultella* and *Aeromonas*. Similarly, the increased prevalence of *Klebsiella* (a potential entomopathogen) in the control mesocosm may result from counterselection in adults harboring this bacterium under PAH exposure (Devi et al., 2022). The increased prevalence of *Aeromonas*, known as an entomopathogen, in the treated mesocosm may indicate dysbiosis favoring opportunistic entomopathogens, particularly in the absence of mediating microbiota taxa such as *Cedecea* or

*Wolbachia*. These hypotheses, supporting the pathogen's presence in PAH-environments, are notably reinforced by the fact that the enriched or depleted taxa (*Klebsiella*, *Aeromonas* and *Cedecea*) belong to the same cluster in our network analysis of mosquito-associated bacterial communities, a cluster that was absent in the control mesocosm. Previous examples suggest that exposure to PAHs could weaken the fitness of adult mosquitoes as mutualistic taxa involved in critical functions are affected. As microbial changes occur within the microbiota, further studies are needed to determine whether PAHs could increase the susceptibility of *Ae. albopictus* mosquitoes to virus infection and affect their sensitivity to insecticides.

Consistent with previous studies, we found that bacterial communities associated with larvae and their breeding sites were highly similar, while adults harbored a divergent microbiota (Coon et al., 2014; Scolari et al., 2021; Zouache et al., 2022). The Comamonadaceae family was the most prevalent bacterial family shared between larvae and water samples. Although they were still detected in adults, their abundance was lower. Members of this family have previously been identified in the larvae and aquatic habitats of field-collected *Ae. albopictus* (Scolari et al., 2021), as well as in other mosquito species like *Ae. aegypti* and *An. gambiae*, along with their rearing environments (Coon et al., 2014; MacLeod et al., 2021). In *Culex nigripalpus,* this family belongs to the core bacterial microbiota that colonizes every life stage (Duguma et al., 2017). Adults showing higher diversity contrast with previous observations in holometabolous insects or even in *Ae. albopictus* (Yun et al., 2014; Scolari et al., 2021; Fu et al., 2023). They may exhibit greater susceptibility to colonization by environmental bacteria, and differences in bacterial composition could be due to the diverse ecological niches they encounter (water, plants, prey) in contrast to larvae, which predominantly inhabit small aquatic habitats. Furthermore, we observed a distinct pattern in larvae over time in both mesocosms. The bacterial communities associated with larvae became more homogeneous over time among individuals, a trend not observed in the water breeding habitats. The reduced variability among larvae could be explained by the selective processes operating within the host microbiota. Indeed, in our context study, larvae are living in a buffered ecosystem with minimal disturbances, suggesting that the primary pressure on larvae arises from intraspecific competition. Consequently, larvae that establish partnerships with selected microbiota over time may be favored, thereby reducing inter-individual microbiota divergence. This phenomenon implies that microbiota could be a significant selective factor under these conditions. However, the homogeneity observed within larval bacterial communities could also be attributed to community drift, where a specific microbiota becomes fixed due to the indoor environment and the limited population size (Gilbert and Levine, 2017).

## 5. Conclusion

This study used indoor mesocosm facilities to investigate how chronic exposure to PAHs affects bacterial dynamics, community shifts and the fate of PAHs within a semi-natural ecosystem. Larvae bioaccumulate PAHs, whereas adults did not, suggesting that no transfer occurred during metamorphosis. A shift in microbiota composition was observed between control and treated mesocosms with an enrichment of bacteria that can thrive in a PAH-contaminated environment. Differential impacts of PAH exposure were also observed according to the development stage of mosquitoes. The inter-individual divergence in bacterial communities decreased over time in larvae but remained unchanged in the aquatic environment and adults. Future studies should investigate how changes in bacterial structure and composition influence mosquito adaptation to PAHs, as previous studies have suggested that microbial communities can modulate host detoxification pathways (Collins and Patterson, 2020; Peterson, 2024). Understanding these dynamics is crucial, given that shifts in microbiota could alter the metabolic capacities of mosquitoes, potentially impacting their survival and reproduction in PAH-contaminated environments. Furthermore, it would be also important to investigate how PAHs impact the host and its microbiota to modify key host functions such as fitness, vector competence, and immunity. Evidence from other studies has demonstrated that microbial diversity can influence immune responses and disease susceptibility in various species (Dennison et al., 2014; Gabrieli et al., 2021; Cai and Christophides, 2024; Destoumieux-Garzón et al., 2024). Therefore, changes in microbiota due to PAH exposure could similarly affect mosquito immunity and vector competence, making this a critical area for future research.

## CRediT authorship contribution statement

**Patrick Mavingui:** Writing – review & editing. **Van Tran Van:** Methodology. **Aymeric Bellemain:** Writing – review & editing, Methodology, Formal analysis. **David Lejon:** Writing – review & editing, Methodology, Conceptualization. **Edwige Martin:** Writing – review & editing, Formal analysis. **Frédéric Simard:** Writing – review & editing. **David Roiz:** Writing – review & editing. **Florence Hélène Tran:** Methodology. **Claire Valiente Moro:** Writing – review & editing, Validation, Supervision, Project administration, Methodology, Funding acquisition, Formal analysis. **Stéphanie Grizard:** Writing – review & editing, Methodology, Formal analysis. **Guillaume Minard:** Writing – review & editing, Supervision. **Pierre Antonelli:** Writing – original draft, Formal analysis. **Aurélien Vigneron:** Writing – review & editing, Supervision. **Danis Abrouk:** Writing – review & editing, Software.

## Declaration of Competing Interest

The authors declare that they have no known competing financial interests or personal relationships that could have appeared to influence the work reported in this paper.

## Acknowledgments

This paper is dedicated to the memory of Florence-Hélène Tran who tragically left us in August 2016. This research was funded by ERA-NET BiodivERsA with the national funders ANR-13-EBID-0007-01, FWF I-1437 and DFG KL 2087/6-1 as part of the 2012–2013 BiodivERsA call for research proposals. We thank Frédéric Darrieux for providing eggs from *Ae. albopictus* mosquito laboratory populations originating from Pérols, France. We also thank the IBIO platform (UMR5557) for providing the computational resources as well as Florence Lamirand for her help in chemical analyses. We also thank Axelle Gentil and Rémy Cazabet for their help for network analyses.

## Appendix A. Supporting information

Supplementary data associated with this article can be found in the online version at doi:10.1016/j.ecoenv.2024.117214.

## Data Availability

I have shared the link in the article

## References

Agrawal, P.K., Shrivastava, R., Verma, J., 2019. Bioremediation approaches for degradation and detoxification of polycyclic aromatic hydrocarbons. In: Bharagava, R.N., Chowdhary, P. (Eds.), In Emerging and Eco-Friendly Approaches for Waste Management. Springer Singapore, Singapore, pp. 99–119.

Albarano, L., Zupo, V., Caramiello, D., Toscanesi, M., Trifuoggi, M., Guida, M., et al., 2021. Sub-chronic effects of slight PAH- and PCB-contaminated mesocosms in *Paracentrotus lividus* Lmk: A multi-endpoint approach and de novo transcriptomic. Int J. Mol. Sci. 22, 6674.

Alegbeleye, O.O., Opeolu, B.O., Jackson, V., 2017. Bioremediation of polycyclic aromatic hydrocarbon (PAH) compounds: (acenaphthene and fluorene) in water using indigenous bacterial species isolated from the Diep and Plankenburg rivers, Western Cape, South Africa. Braz. J. Microbiol 48, 314–325.

Algamdi, A.G., Shaher, F.M., Mahyoub, J.A., 2023. Biological comparative study between *Wolbachia*-infected *Aedes aegypti* mosquito and *Wolbachia*-uninfected strain, Jeddah city, Saudi Arabia. Saudi J. Biol. Sci. 30, 103581.
Ali, H., Khan, E., Ilahi, I., 2019. Environmental chemistry and ecotoxicology of hazardous heavy metals: environmental persistence, toxicity, and bioaccumulation. J. Chem. 2019, 6730305.
Al-Jaibachi, R., Cuthbert, R.N., Callaghan, A., 2019. Examining effects of ontogenic microplastic transference on *Culex* mosquito mortality and adult weight. Sci. Total Environ. 651, 871–876.
Antonelli, P., Duval, P., Luis, P., Minard, G., Valiente Moro, C., 2022. Reciprocal interactions between anthropogenic stressors and insect microbiota. Environ. Sci. Pollut. Res 29, 64469–64488.
Aoki, Y., Suzuki, K.T., 1984. Excretion of cadmium and change in the relative ratio of iso-cadmium-binding proteins during metamorphosis of fleshfly (*Sarcophaga peregrina*). Comp. Biochem Physiol. C. Comp. Pharm. Toxicol. 78, 315–317.
Aziz, K.H.H., Mustafa, F.S., Omer, K.M., Hama, S., Hamarawf, R.F., Rahman, K.O., 2023. Heavy metal pollution in the aquatic environment: efficient and low-cost removal approaches to eliminate their toxicity: a review. RSC Adv. 13, 17595–17610.
Baldantoni, D., Morelli, R., Bellino, A., Prati, M.V., Alfani, A., De Nicola, F., 2017. Anthracene and benzo(a)pyrene degradation in soil is favoured by compost amendment: Perspectives for a bioremediation approach. J. Hazard Mater. 339, 395–400.
Bartrons, M., Grimalt, J.O., Catalan, J., 2007. Concentration changes of organochlorine compounds and polybromodiphenyl ethers during metamorphosis of aquatic insects. Environ. Sci. Technol. 41, 6137–6141.
Bastian, M., Heymann, S., Jacomy, M., 2009. Gephi: An open source software for exploring and manipulating networks. Proc. Int. AAAI Conf. Web Soc. Media 3, 361–362.
Bernard, M., Rué, O., Mariadassou, M., Pascal, G., 2021. FROGS: a powerful tool to analyse the diversity of fungi with special management of internal transcribed spacers. Brief. Bioinforma. 22, bbab318.
Biessy, A., Ciotola, M., Cadieux, M., Albert, D., Filion, M., 2022. Genome sequences of two soil-dwelling bacteria belonging to the family Comamonadaceae. Microbiol Resour. Announc 11, e0023022.
Bikis, A., 2023. Urban air pollution and greenness in relation to public health. J. Environ. Public Health 2023, 8516622.
Bokulich, N.A., Subramanian, S., Faith, J.J., Gevers, D., Gordon, J.I., Knight, R., et al., 2013. Quality-filtering vastly improves diversity estimates from Illumina amplicon sequencing. Nat. Methods 10, 57–59.
Bonizzoni, M., Gasperi, G., Chen, X., James, A.A., 2013. The invasive mosquito species *Aedes albopictus*: current knowledge and future perspectives. Trends Parasitol. 29, 460–468.
Bravo, C.F., Curtis, L.R., Myers, M.S., Meador, J.P., Johnson, L.L., Buzitis, J., et al., 2011. Biomarker responses and disease susceptibility in juvenile rainbow trout *Oncorhynchus mykiss* fed a high molecular weight PAH mixture. Environ. Toxicol. Chem. 30, 704–714.
Brennan, L.J., Keddie, B.A., Braig, H.R., Harris, H.L., 2008. The endosymbiont *Wolbachia pipientis* induces the expression of host antioxidant proteins in an *Aedes albopictus* cell line. PLOS ONE 3, e2083.
Cai, J.A., Christophides, G.K., 2024. Immune interactions between mosquitoes and microbes during midgut colonization. Curr. Opin. Insect Sci. 63, 101195.
Cappelli, A., Damiani, C., Mancini, M.V., Valzano, M., Rossi, P., Serrao, A., et al., 2019. *Asaia* activates immune genes in mosquito eliciting an anti-*Plasmodium* response: implications in malaria Control. Front Genet 10, 836.
Caragata, E.P., Otero, L.M., Tikhe, C.V., Barrera, R., Dimopoulos, G., 2022. Microbial diversity of adult *Aedes aegypti* and water collected from different mosquito aquatic habitats in Puerto Rico. Micro Ecol. 83, 182–201.
Chaix, G., Roger, F., Berthe, T., Lamy, B., Jumas-Bilak, E., Lafite, R., et al., 2017. Distinct *Aeromonas* populations in water column and associated with copepods from estuarine environment (Seine, France). Front. Microbiol. 8.
Choo, M.Z.J., Low, B.W., Ngiam, R.W.J., Yeo, D.C.J., 2021. Predation of mosquitos by odonates in a tropical urban environment: insights from functional response and field mesocosm experiments. Biol. Control 161, 104702.
Collins, S.L., Patterson, A.D., 2020. The gut microbiome: an orchestrator of xenobiotic metabolism. Acta Pharm. Sin. B 10, 19–32.
Comandatore, F., Damiani, C., Cappelli, A., Ribolla, P.E.M., Gasperi, G., Gradoni, F., et al., 2021. Phylogenomics reveals that *Asaia* symbionts from insects underwent convergent genome reduction, preserving an insecticide-degrading gene. mBio 12, e00106–e00121.
Coon, K.L., Brown, M.R., Strand, M.R., 2016. Gut bacteria differentially affect egg production in the anautogenous mosquito *Aedes aegypti* and facultatively autogenous mosquito *Aedes atropalpus* (Diptera: Culicidae). Parasit. Vectors 9, 375.
Coon, K.L., Vogel, K.J., Brown, M.R., Strand, M.R., 2014. Mosquitoes rely on their gut microbiota for development. Mol. Ecol. 23, 2727–2739.
R. Core Team 2022 R: A language and environment for statistical computing. R Foundation for Statistical Computing, Vienna, Austria. URL ⟨https://www.R-project.org/⟩.
Cui, Z., Wang, Y., Du, L., Yu, Y., 2022. Contamination level, sources, and health risk of polycyclic aromatic hydrocarbons in suburban vegetable field soils of Changchun, Northeast China. Sci. Rep. 12, 11301.
Cui, G., Zhong, S., Zheng, T., Li, Z., Zhang, X., Li, C., et al., 2021. *Aedes albopictus* life table: environment, food, and age dependence survivorship and reproduction in a tropical area. Parasites Vectors 14, 568.
Curtis, L.R., Bravo, C.F., Bayne, C.J., Tilton, F., Arkoosh, M.R., Lambertini, E., et al., 2017. Transcriptional changes in innate immunity genes in head kidneys from *Aeromonas salmonicida*-challenged rainbow trout fed a mixture of polycyclic aromatic hydrocarbons. Ecotoxicol. Environ. Saf. 142, 157–163.
Dada, N., Benedict, A.C., López, F., Lol, J.C., Sheth, M., Dzuris, N., et al., 2021. Comprehensive characterization of internal and cuticle surface microbiota of laboratory-reared F1 *Anopheles albimanus* originating from different sites. Malar. J. 20, 414.
Daisley, B.A., Trinder, M., McDowell, T.W., Welle, H., Dube, J.S., Ali, S.N., et al., 2017. Neonicotinoid-induced pathogen susceptibility is mitigated by *Lactobacillus plantarum* immune stimulation in a *Drosophila melanogaster* model. Sci. Rep. 7, 2703.
David, M.R., Santos, L.M.B.D., Vicente, A.C.P., Maciel-de-Freitas, R., 2016. Effects of environment, dietary regime and ageing on the dengue vector microbiota: evidence of a core microbiota throughout *Aedes aegypti* lifespan. Mem. Inst. Oswaldo Cruz 111, 577–587.
Dellar, M., Boerlijst, S.P., Holmes, D., 2022. Improving estimations of life history parameters of small animals in mesocosm experiments: A case study on mosquitoes. Methods Ecol. Evol. 13, 1148–1160.
Dennison, N.J., Jupatanakul, N., Dimopoulos, G., 2014. The mosquito microbiota influences vector competence for human pathogens. Curr. Opin. Insect Sci. 3, 6–13.
Destoumieux-Garzón, D., Montagnani, C., Dantan, L., Nicolas, N. de S., Travers, M.-A., Duperret, L., et al., 2024. Cross-talk and mutual shaping between the immune system and the microbiota during an oyster's life. Philos. Trans. R. Soc. Lond. B Biol. Sci. 379, 20230065.
Devi, S., Saini, H.S., Kaur, S., 2022. Insecticidal and growth inhibitory activity of gut microbes isolated from adults of *Spodoptera litura* (Fab.). BMC Microbiol 22, 71.
Díaz-Nieto, L.M., D'Alessio, C., Perotti, M.A., Berón, C.M., 2016. *Culex pipiens* development is greatly influenced by native bacteria and exogenous yeast. PLoS One 11, e0153133.
Dickens, B.L., Sun, H., Jit, M., Cook, A.R., Carrasco, L.R., 2018. Determining environmental and anthropogenic factors which explain the global distribution of *Aedes aegypti* and *Ae. albopictus*. BMJ Glob. Health 3, e000801.
Dong, Y., Wu, S., Fan, H., Li, X., Li, Y., Xu, S., et al., 2022. Ecological selection of bacterial taxa with larger genome sizes in response to polycyclic aromatic hydrocarbons stress. J. Environ. Sci. 112, 82–93.
Dubey, S., Ager-Wick, E., Kumar, J., Karunasagar, Indrani, Karunasagar, Iddya, Peng, B., et al., 2022. *Aeromonas* species isolated from aquatic organisms, insects, chicken, and humans in India show similar antimicrobial resistance profiles. Front Microbiol 13, 1008870.
Duguma, D., Hall, M.W., Smartt, C.T., Neufeld, J.D., 2017. Effects of organic amendments on microbiota associated with the *Culex nigripalpus* mosquito vector of the Saint Louis encephalitis and West Nile viruses. mSphere 2, e00387-16.
Duval, P., Antonelli, P., Aschan-Leygonie, C., Valiente Moro, C., 2023. Impact of human activities on disease-spreading mosquitoes in urban areas. J. Urban Health.
Escudié, F., Auer, L., Bernard, M., Mariadassou, M., Cauquil, L., Vidal, K., et al., 2018. FROGS: Find, Rapidly, OTUs with Galaxy Solution. Bioinformatics 34, 1287–1294.
Fox J., Weisberg S. 2019 An R companion to applied regression, Third edition. Sage, Thousand Oaks CA.
Fruchterman, T.M.J., Reingold, E.M., 1991. Graph drawing by force-directed placement. Softw.: Pract. Exp. 21, 1129–1164.
Fu, J., Wang, J., Huang, X., Guan, B., Feng, Q., Deng, H., 2023. Composition and diversity of gut microbiota across developmental stages of *Spodoptera frugiperda* and its effect on the reproduction. Front Microbiol 14.
Ga'al, H., Fouad, H., Tian, J., Hu, Y., Abbas, G., Mo, J., 2018. Synthesis, characterization and efficacy of silver nanoparticles against *Aedes albopictus* larvae and pupae. Pest. Biochem Physiol. 144, 49–56.
Gabrieli, P., Caccia, S., Varotto-Boccazzi, I., Arnoldi, I., Barbieri, G., Comandatore, F., Epis, S., 2021. Mosquito trilogy: microbiota, immunity and pathogens, and their implications for the control of disease transmission. Front Microbiol 12, 630438.
Garagnon, J., Perrette, Y., Naffrechoux, E., Pons-Branchu, E., 2023. Polycyclic aromatic hydrocarbon record in an urban secondary carbonate deposit over the last three centuries (Paris, France). Sci. Total Environ. 905, 167429.
Gilbert, B., Levine, J.M., 2017. Ecological drift and the distribution of species diversity. Proc. R. Soc. B: Biol. Sci. 284, 20170507.
Girardin, V., Grung, M., Meland, S., 2020. Polycyclic aromatic hydrocarbons: bioaccumulation in dragonfly nymphs (Anisoptera), and determination of alkylated forms in sediment for an improved environmental assessment. Sci. Rep. 10, 10958.
Griffin, C.D., Tominiko, C., Medeiros, M.C.I., Walguarnery, J.W., 2023. Microplastic pollution differentially affects development of disease-vectoring *Aedes* and *Culex* mosquitoes. Ecotoxicol. Environ. Saf. 267, 115639.
Gu, Z., 2022. Complex heatmap visualization. iMeta 1, e43.
Guzman, M.G., Halstead, S.B., Artsob, H., Buchy, P., Farrar, J., Gubler, D.J., et al., 2010. Dengue: a continuing global threat. Nat. Rev. Microbiol 8, S7–S16.
Hare, L., 1992. Aquatic insects and trace metals: bioavailability, bioaccumulation, and toxicity. Crit. Rev. Toxicol. 22, 327–369.
Hartig, F. (2022) *DHARMa: Residual Diagnostics for Hierarchical (Multi-Level / Mixed) Regression Models*.
Hegde, S., Nilyanimit, P., Kozlova, E., Anderson, E.R., Narra, H.P., Sahni, S.K., et al., 2019. CRISPR/Cas9-mediated gene deletion of the ompA gene in symbiotic *Cedecea neteri* impairs biofilm formation and reduces gut colonization of *Aedes aegypti* mosquitoes. PLoS Negl. Trop. Dis. 13, e0007883.
Hem, S., Wyrsch, E.R., Drigo, B., Baker, D.J., Charles, I.G., Donner, E., et al., 2022. Genomic analysis of carbapenem-resistant *Comamonas* in water matrices: Implications for public health and wastewater treatments. Appl. Environ. Microbiol 88, e0064622.
Hierlmeier, V.R., Gurten, S., Freier, K.P., Schlick-Steiner, B.C., Steiner, F.M., 2022. Persistent, bioaccumulative, and toxic chemicals in insects: Current state of research and where to from here? Sci. Total Environ. 825, 153830.

Honda, M., Suzuki, N., 2020. Toxicities of polycyclic aromatic hydrocarbons for aquatic animals. Int J. Environ. Res Public Health 17, 1363.
Huang, L.-Q., Luo, X.-J., Qi, X.-M., Mai, B.-X., 2020. Sex-specific bioamplification of halogenated organic pollutants during silkworm (*Bombyx mori*) metamorphosis and their adverse effects on silkworm development. Environ. Sci. Technol. 54, 8167–8176.
Hussain, K., Hoque, R.R., Balachandran, S., Medhi, S., Idris, M.G., Rahman, M., Hussain, F.L., 2018. Monitoring and risk analysis of PAHs. In: Hussain, C.M. (Ed.), the Environment. In *Handbook of Environmental Materials Management*. Springer International Publishing, Cham, pp. 1–35.
Jackson, E., Shoemaker, R., Larian, N., Cassis, L., 2017. Adipose tissue as a site of toxin accumulation. *Compr. Physiol.* 7 1085–1135.
Jesus, F., Pereira, J.L., Campos, I., Santos, M., Ré, A., Keizer, J., et al., 2022. A review on polycyclic aromatic hydrocarbons distribution in freshwater ecosystems and their toxicity to benthic fauna. Sci. Total Environ. 820, 153282.
Johnson, K.N., 2015. The Impact of *Wolbachia* on virus infection in mosquitoes. Viruses 7, 5705–5717.
Kolimenakis, A., Heinz, S., Wilson, M.L., Winkler, V., Yakob, L., Michaelakis, A., et al., 2021. The role of urbanisation in the spread of *Aedes* mosquitoes and the diseases they transmit—A systematic review. PLoS Negl. Trop. Dis. 15, e0009631.
Kozlov, M.V., 2022. Population dynamics of herbivorous insects in polluted landscapes. Curr. Opin. Insect Sci. 54, 100987.
Kozlova, E.V., Hegde, S., Roundy, C.M., Golovko, G., Saldaña, M.A., Hart, C.E., et al., 2021. Microbial interactions in the mosquito gut determine *Serratia* colonization and blood-feeding propensity. ISME J. 15, 93–108.
Kraemer, M.U.G., Reiner, R.C., Brady, O.J., Messina, J.P., Gilbert, M., Pigott, D.M., et al., 2019. Past and future spread of the arbovirus vectors *Aedes aegypti* and *Aedes albopictus*. Nat. Microbiol 4, 854–863.
Kraus, J.M., Walters, D.M., Wesner, J.S., Stricker, C.A., Schmidt, T.S., Zuellig, R.E., 2014. Metamorphosis alters contaminants and chemical tracers in insects: implications for food webs. Environ. Sci. Technol. 48, 10957–10965.
Kyritsis, G.A., Augustinos, A.A., Cáceres, C., Bourtzis, K., 2017. Medfly gut microbiota and enhancement of the sterile insect technique: Similarities and differences of *Klebsiella oxytoca* and Enterobacter sp. AA26 probiotics during the larval and adult Stages of the VIENNA 8D53+ genetic sexing strain. Front Microbiol 8, 2064.
Lacour, G., Chanaud, L., L'Ambert, G., Hance, T., 2015. Seasonal synchronization of diapause phases in *Aedes albopictus* (Diptera: Culicidae). PLOS ONE 10, e0145311.
Lambert, O., Veyrand, B., Durand, S., Marchand, P., Bizec, B.L., Piroux, M., et al., 2012. Polycyclic aromatic hydrocarbons: Bees, honey and pollen as sentinels for environmental chemical contaminants. Chemosphere 86, 98–104.
Lawton, J.H., 1996. The ecotron facility at Silwood Park: The value of "Big Bottle" experiments. Ecology 77, 665–669.
Lenth R.V. 2023 emmeans: Estimated Marginal Means, aka Least-Squares Means_.
Leta, S., Beyene, T.J., De Clercq, E.M., Amenu, K., Kraemer, M.U.G., Revie, C.W., 2018. Global risk mapping for major diseases transmitted by *Aedes aegypti* and *Aedes albopictus*. Int J. Infect. Dis. 67, 25–35.
Liang, L., Gong, P., 2020. Urban and air pollution: a multi-city study of long-term effects of urban landscape patterns on air quality trends. Sci. Rep. 10, 18618.
Liu, Y., Luo, X.-J., Huang, L.-Q., Yu, L.-H., Mai, B.-X., 2018. Bioaccumulation of persistent halogenated organic pollutants in insects: Common alterations to the pollutant pattern for different insects during metamorphosis. Environ. Sci. Technol. 52, 5145–5153.
Liu, Y., Luo, X., Zeng, Y., Wang, Q., Tu, W., Yang, C., Mai, B., 2020. Trophic magnification of short- and medium-chain chlorinated paraffins in terrestrial food webs and their bioamplification in insects and amphibians during metamorphosis. Environ. Sci. Technol. 54, 11282–11291.
Liu, Y., Zarfl, C., Basu, N.B., Cirpka, O.A., 2019. Turnover and legacy of sediment-associated PAH in a baseflow-dominated river. Sci. Total Environ. 671, 754–764.
Lowe S., Browne M., Boudjelas S., and De Poorter M. (2004) 100 of the World's worst invasive alien species a selection from the Global Invasive Species Database.
Luoma, S.N., Rainbow, P.S., 2005. Why is metal bioaccumulation so variable? Biodynamics as a unifying concept. Environ. Sci. Technol. 39, 1921–1931.
Ma, Q., Han, X., Song, J., Wang, J., Li, Q., Parales, R.E., et al., 2023. Characterization of a new chlorimuron-ethyl-degrading strain *Cedecea* sp. LAM2020 and biodegradation pathway revealed by multiomics analysis. J. Hazard. Mater. 443, 130197.
MacLeod, H.J., Dimopoulos, G., Short, S.M., 2021. Larval diet abundance influences size and composition of the midgut microbiota of *Aedes aegypti* mosquitoes. Front Microbiol 12, 645362.
Manisalidis, I., Stavropoulou, E., Stavropoulos, A., Bezirtzoglou, E., 2020. Environmental and health impacts of air pollution: A review. Front Public Health 8.
Mariño, Y.A., Verle Rodrigues, J.C., Bayman, P., 2017. *Wolbachia* affects reproduction and population dynamics of the coffee berry borer (*Hypothenemus hampei*): Implications for biological control. Insects 8, 8.
McMurdie, P.J., Holmes, S., 2013. phyloseq: An R package for reproducible interactive analysis and graphics of microbiome census data. PLOS ONE 8, e61217.
Medlock, J.M., Hansford, K.M., Versteirt, V., Cull, B., Kampen, H., Fontenille, D., et al., 2015. An entomological review of invasive mosquitoes in Europe. Bull. Èntomol. Res. 105, 637–663.
Minard, G., Tran, F.H., Van, V.T., Goubert, C., Bellet, C., Lambert, G., et al., 2015. French invasive Asian tiger mosquito populations harbor reduced bacterial microbiota and genetic diversity compared to Vietnamese autochthonous relatives. Front Microbiol 6, 970.
Moser, R., Stahl, U., 2001. Insights into the genetic diversity of initial dioxygenases from PAH-degrading bacteria. Appl. Microbiol Biotechnol. 55, 609–618.
Ng'habi, K., Viana, M., Matthiopoulos, J., Lyimo, I., Killeen, G., Ferguson, H.M., 2018. Mesocosm experiments reveal the impact of mosquito control measures on malaria vector life history and population dynamics. Sci. Rep. 8, 13949.
Noonin, C., Jiravanichpaisal, P., Söderhäll, I., Merino, S., Tomás, J.M., Söderhäll, K., 2010. Melanization and pathogenicity in the insect, *Tenebrio molitor*, and the crustacean, *Pacifastacus ieniusculus*, by *Aeromonas hydrophila* AH-3. PLOS ONE 5, e15728.
Oksanen, J., Blanchet, F.G., Kindt, R., Legendre, P., Minchin, P., O'Hara, B., et al., 2015. Vegan: community ecology package. R. Package Version 22-1 2, 1–2.
Olkeba, B.K., Goethals, P.L.M., Boets, P., Duchateau, L., Degefa, T., Eba, K., et al., 2021. Mesocosm experiments to quantify predation of mosquito larvae by aquatic predators to determine potential of ecological control of malaria vectors in Ethiopia. Int J. Environ. Res Public Health 18, 6904.
Patel, A.B., Shaikh, S., Jain, K.R., Desai, C., Madamwar, D., 2020. Polycyclic aromatic hydrocarbons: Sources, toxicity, and remediation approaches. Front Microbiol 11, 562813.
Paupy, C., Delatte, H., Bagny, L., Corbel, V., Fontenille, D., 2009. *Aedes albopictus*, an arbovirus vector: from the darkness to the light. Microbes Infect. 11, 1177–1185.
Pelloquin, B., Kristan, M., Edi, C., Meiwald, A., Clark, E., Jeffries, C.L., et al., 2021. Overabundance of *Asaia* and *Serratia* bacteria is associated with deltamethrin insecticide susceptibility in *Anopheles coluzzii* from Agboville, Côte d'Ivoire. Microbiol Spectr. 9, e0015721.
Peng, R.-H., Xiong, A.-S., Xue, Y., Fu, X.-Y., Gao, F., Zhao, W., et al., 2008. Microbial biodegradation of polyaromatic hydrocarbons. FEMS Microbiol. Rev. 32, 927–955.
Perugini, M., Di Serafino, G., Giacomelli, A., Medrzycki, P., Sabatini, A.G., Persano Oddo, L., et al., 2009. Monitoring of polycyclic aromatic hydrocarbons in bees (*Apis mellifera*) and honey in urban areas and wildlife reserves. J. Agric. Food Chem. 57, 7440–7444.
Peterson, B.F., 2024. Microbiome toxicology — bacterial activation and detoxification of insecticidal compounds. Curr. Opin. Insect Sci. 63, 101192.
Petrović, J., Kartalović, B., Ratajac, R., Spirić, D., Djurdjević, B., Polaček, V., Pucarević, M., 2019. PAHs in different honeys from Serbia. Food Addit. Contam. Part B Surveill. 12, 116–123.
Pfannkoch, E.A., Stuff, J.R., Whitecavage, J.A., Blevins, J.M., Seely, K.A., Moran, J.H., 2015. A high throughput method for measuring polycyclic aromatic hydrocarbons in seafood using QuEChERS extraction and SBSE. Int. J. Anal. Chem. 2015, 359629.
Ping, L., Guo, Q., Chen, X., Yuan, X., Zhang, C., Zhao, H., 2017. Biodegradation of pyrene and benzo[a]pyrene in the liquid matrix and soil by a newly identified *Raoultella planticola* strain. 3 Biotech 7, 56.
Pölkki, M., Kangassalo, K., Rantala, M.J., 2012. Transgenerational effects of heavy metal pollution on immune defense of the blow fly *Protophormia terraenovae*. PLOS ONE 7, e38832.
Poupardin, R., Reynaud, S., Strode, C., Ranson, H., Vontas, J., David, J.-P., 2008. Cross-induction of detoxification genes by environmental xenobiotics and insecticides in the mosquito *Aedes aegypti*: impact on larval tolerance to chemical insecticides. Insect Biochem Mol. Biol. 38, 540–551.
Quast, C., Pruesse, E., Yilmaz, P., Gerken, J., Schweer, T., Yarza, P., et al., 2013. The SILVA ribosomal RNA gene database project: improved data processing and web-based tools. Nucleic Acids Res. 41, D590–D596.
Ramkumar, G., Muthusamy, R., Narayanan, M., Dhanapal, R., Karthik, C., Shivakumar, M.S., et al., 2022. Pretreatment of mosquito larvae with ultraviolet-B and nitropolycyclic aromatic hydrocarbons induces increased sensitivity to permethrin toxicity. Heliyon 8, e11094.
Rhodes, Gerald, Opsal, R.B., Meek, J.T., Reilly, J.P., 1983. Analysis of polyaromatic hydrocarbon mixtures with laser ionization gas chromatography/mass spectrometry. Anal. Chem. 55, 280–286.
Ribière, C., Peyret, P., Parisot, N., Darcha, C., Déchelotte, P.J., Barnich, N., et al., 2016. Oral exposure to environmental pollutant benzo[a]pyrene impacts the intestinal epithelium and induces gut microbial shifts in murine model. Sci. Rep. 6, 31027.
Rognes, T., Flouri, T., Nichols, B., Quince, C., Mahé, F., 2016. VSEARCH: a versatile open source tool for metagenomics. PeerJ 4, e2584.
Roiz, D., Pontifes, P.A., Jourdain, F., Diagne, C., Leroy, B., Vaissière, A.-C., et al., 2024. The rising global economic costs of invasive *Aedes* mosquitoes and *Aedes*-borne diseases. Sci. Total Environ. 933, 173054.
Ryalls, J.M.W., Bishop, J., Mofikoya, A.O., Bromfield, L.M., Nakagawa, S., Girling, R.D., 2024. Air pollution disproportionately impairs beneficial invertebrates: a meta-analysis. Nat. Commun. 15, 5447.
Ryan, S.J., Carlson, C.J., Mordecai, E.A., Johnson, L.R., 2019. Global expansion and redistribution of *Aedes*-borne virus transmission risk with climate change. PLOS Negl. Trop. Dis. 13, e0007213.
Sampaio, G.R., Guizellini, G.M., da Silva, S.A., de Almeida, A.P., Pinaffi-Langley, A.C.C., Rogero, M.M., et al., 2021. Polycyclic aromatic hydrocarbons in foods: Biological effects, legislation, occurrence, analytical methods, and strategies to reduce their formation. Int J. Mol. Sci. 22, 6010.
Scolari, F., Sandionigi, A., Carlassara, M., Bruno, A., Casiraghi, M., Bonizzoni, M., 2021. Exploring changes in the microbiota of *Aedes albopictus*: Comparison among breeding site water, larvae, and adults. Front Microbiol 12, 624170.
Smith, D.F.Q., Camacho, E., Thakur, R., Barron, A.J., Dong, Y., Dimopoulos, G., et al., 2021. Glyphosate inhibits melanization and increases susceptibility to infection in insects. PLoS Biol. 19, e3001182.
Soltani, A., Vatandoost, H., Oshaghi, M., Enayati, A., Chavshin, A.R., 2017. The role of midgut symbiotic bacteria in resistance of *Anopheles stephensi* (Diptera: Culicidae) to organophosphate insecticides. Pathog. Glob. Health 111, 1–8.
Straw, E.A., Mesnage, R., Brown, M.J.F., Antoniou, M.N., 2023. No impacts of glyphosate or *Crithidia bombi*, or their combination, on the bumblebee microbiome. Sci. Rep. 13, 8949.

Sun, Y., Tian, Y., Xue, Q., Jia, B., Wei, Y., Song, D., et al., 2021. Source-specific risks of synchronous heavy metals and PAHs in inhalable particles at different pollution levels: Variations and health risks during heavy pollution. Environ. Int. 146, 106162.

Tetreau, G., Chandor-Proust, A., Faucon, F., Stalinski, R., Akhouayri, I., Prud'homme, S. M., et al., 2014. UV light and urban pollution: bad cocktail for mosquitoes? Aquat. Toxicol. 146, 52–60.

Thompson, D.K., Sharkady, S.M., 2020. Expanding spectrum of opportunistic *Cedecea* infections: Current clinical status and multidrug resistance. Int. J. Infect. Dis. 100, 461–469.

Trzebny, A., Slodkowicz-Kowalska, A., Björkroth, J., Dabert, M., 2023. Microsporidian infection in mosquitoes (Culicidae) is associated with gut microbiome composition and predicted gut microbiome functional content. Micro Ecol. 85, 247–263.

van der Loos, L.M., D'hondt, S., Engelen, A.H., Pavia, H., Toth, G.B., Willems, A., et al., 2023. Salinity and host drive *Ulva*-associated bacterial communities across the Atlantic-Baltic sea gradient. Mol. Ecol. 32, 6260–6277.

Wesner, J., Kraus, J.M., Henry, B.L., and Kerby, J. (2020) Metamorphosis and the impact of contaminants on ecological subsidies. 111–125.

Wickham, H., 2016. ggplot2. Springer International Publishing, Cham.

Xie, M., Zhang, S., Xu, L., Wu, Z., Yuan, J., Chen, X., 2021. Comparison of the intestinal microbiota during the different growth stages of red swamp crayfish (*Procambarus clarkii*). Front Microbiol 12, 696281.

Xie, S., Zhou, A., Xu, N., Feng, Y., Pan, Z., Junaid, M., et al., 2020. Benzo[a]pyrene induces microbiome dysbiosis and inflammation in the intestinal tracts of western mosquitofish (*Gambusia affinis*) and zebrafish (*Danio rerio*). Fish. Shellfish Immunol. 105, 24–34.

Yin, Y., Wang, S., Zhang, K., Li, Y., Liu, W., Zhang, Q., et al., 2023. *Klebsiella pneumoniae* in the intestines of *Musca domestica* larvae can assist the host in antagonizing the poisoning of the heavy metal copper. BMC Microbiol. 23, 383.

Yu, L., Chen, X., Wei, Y., Ding, Y., Wang, Q., Wang, Shaohua, et al., 2020. Effects of long-term cadmium exposure on trehalose metabolism, growth, and development of *Aedes albopictus* (Diptera: Culicidae). Ecotoxicol. Environ. Saf. 204, 111034.

Yun, J.-H., Roh, S.W., Whon, T.W., Jung, M.-J., Kim, M.-S., Park, D.-S., et al., 2014. Insect gut bacterial diversity determined by environmental habitat, diet, developmental stage, and phylogeny of host. Appl. Environ. Microbiol 80, 5254–5264.

Zhang, W., Sun, Z., Zhang, Q., et al., 2021. Preliminary evidence for an influence of exposure to polycyclic aromatic hydrocarbons on the composition of the gut microbiota and neurodevelopment in three-year-old healthy children. BMC Pediatr 21, 86. https://doi.org/10.1186/s12887-021-02539-w.

Zhao, Y., Liu, H., Wang, Q., Li, B., Zhang, H., Pi, Y., 2019. The effects of benzo[a]pyrene on the composition of gut microbiota and the gut health of the juvenile sea cucumber *Apostichopus japonicus* Selenka. ISSN 1050-4648 Fish Shellfish Immunol. 93, 369–379. https://doi.org/10.1016/j.fsi.2019.07.073.

Zhou, C., Huang, J.-C., Zheng, L., He, S., Zhou, W., 2020. Trophic transfer and biotransformation of selenium in the mosquito (*Aedes albopictus*) and interactive effects with hexavalent chromium. Environ. Pollut. 262, 114288.

Zouache, K., Martin, E., Rahola, N., Gangue, M.F., Minard, G., Dubost, A., et al., 2022. Larval habitat determines the bacterial and fungal microbiota of the mosquito vector *Aedes aegypti*. FEMS Microbiol Ecol. 98, fiac016.